Flexibility and profitability quantification for an aggregation of EVs providing frequency services

Author:
Julian Marius Mittag
DTU Wind-M-0810
July 2024

Author:
Julian Marius Mittag

Title:
Flexibility and profitability quantification for an aggregation of EVs providing frequency services

DTU Wind-M-0810

July 2024

ECTS: 35

Education: Master of Science

Supervisors:
Mattia Marinelli
Jan M. W. Zepter
Mattia Secchi
Anna Malkova
DTU Wind & Energy Systems

Remarks:
This report is submitted as partial fulfillment of the requirements for graduation in the above education at the Technical University of Denmark.

DTU Wind & Energy Systems is a department of the Technical University of Denmark with a unique integration of research, education, innovation and public/private sector consulting in the field of wind energy. Our activities develop new opportunities and technology for the global and Danish exploitation of wind energy. Research focuses on key technical-scientific fields, which are central for the development, innovation and use of wind energy and provides the basis for advanced education at the education.

Technical University of Denmark
Department of Wind and Energy Systems
Frederiksborgvej 399
DK-4000 Roskilde
Denmark
www.wind.dtu.dk

Approval

This thesis has been prepared over six months at the Section for E-mobility and Prosumer Integration, Department of Wind and Energy Systems, at the Technical University of Denmark, DTU, in partial fulfilment for the degree Master of Science in Sustainable Energy, MSc Eng.

It is assumed that the reader has a basic knowledge in the areas of electric power grids and markets, machine learning and linear programming.

Julian Marius Mittag - s222781

Signature

July 22, 2024

Date

Abstract

The energy transition, which includes the integration of renewable energy and carbon-free technologies like electric vehicles (EVs), is steadily transforming the energy landscape. This shift presents various challenges for power systems but also offers opportunities. In this thesis, it is explored how EVs can provide flexibility by offering frequency services. It examines current ancillary service regulations in the Nordics and analyzes frequency service markets to identify trends and patterns. A machine learning approach is used to develop a load forecasting model for EV charging processes. Additionally, a decision model based on linear programming is created to optimally allocate forecasted capacities to the two frequency services Frequency Containment Reserve for Disturbance Operation (FCR-D) and Fast Frequency Response (FFR).

The models are applied to a case study, in which a workspace parking lot with 12 EV charging points at the Technical University of Denmark is considered. From this real-world data, 30 artificial parking lots with similar characteristics are created. The study investigates the profitability of offering capacities according to a) the historical 10^{th} quantile per hour per day, which is referred to as baseline, b) day-ahead load predictions using machine learning, c) load predictions for a hypothetical market structure, where the late FCR-D auction is treated as an intraday auction with a gate-closure time one hour before operation and d) perfect foresight of charging loads and market prices.

The study finds that participation in FFR is low, because the charging patterns of the workday parking lot do not align with FFR demand. Offering bids according to the statistical 10^{th} quantile baseline yields an annual revenue of 13.88 € per outlet for the considered parking lot. Using machine learning forecasts instead of the baseline, the profitability is increased to 25.38 € per outlet. The hypothetical market structure significantly improves EV profitability in frequency services by allowing closer to real-time bidding, thus enhancing forecast accuracy of the machine learning model. This scenario finds an annual profit of 77.89 € per outlet. Finally, by considering perfect foresight, a profit ceiling of 176.18 € per outlet per year is established, representing the maximum expected revenue.

Acknowledgements

This work was financially supported by by the European Union's Horizon 2020 research and innovation programme through the research projects FLOW (Flexible energy systems Leveraging the Optimal integration of EVs deployment Wave) and EV4EU (Electric Vehicles Management for carbon neutrality in Europe), under grant agreement No. 101056730 and 101056765.

I would like to sincerely thank my supervisors Mattia, Jan Martin, Mattia and Anna for their continuous support and guidance throughout the thesis project.

Contents

List of Figures

List of Tables

Nomenclature

	Symbol	Set
Decision Variables		
FCR-D up bid in the early auction in hour t	$p_{t^{\text{up-e}}}$	$\forall t \in \mathcal{T}$
FCR-D up bid in the late auction in hour t	$p_{t^{\text{up-t}}}$	$\forall t \in \mathcal{T}$
FCR-D down bid in the early auction in hour t	$p_t^{\text{down-e}}$	$\forall t \in \mathcal{T}$
FCR-D down bid in the late auction in hour t	$p_t^{\text{down-t}}$	$\forall t \in \mathcal{T}$
Preliminary FFR bid in the early auction in hour t	$p_t^{\text{FFR-prelim}}$	$\forall t \in \mathcal{T}$
FFR bid in hour t	p_t^{FFR}	$\forall t \in \mathcal{T}$
Auxiliary variable for LER linearisation in hour t	aux_t^{up}	$\forall t \in \mathcal{T}$
Auxiliary variable for LER linearisation in hour t	aux_t^{down}	$\forall t \in \mathcal{T}$
Binary variable for LER linearisation in hour t	y_t^{up}	$\forall t \in \mathcal{T}$
Binary variable for LER linearisation in hour t	y_t^{down}	$\forall t \in \mathcal{T}$
Parameters		
FCR-D up price expectation in the early auction in hour t	λ_t^{up-e}	$\forall t \in \mathcal{T}$
FCR-D up price expectation in the late auction in hour t	λ_t^{up-l}	$\forall t \in \mathcal{T}$
FCR-D down price expectation in the early auction in hour t	λ_t^{down-e}	$\forall t \in \mathcal{T}$
FCR-D down price expectation in the late auction in hour t	λ_t^{down-l}	$\forall t \in \mathcal{T}$
FFR price expectation in hour t	λ_t^{FFR}	$\forall t \in \mathcal{T}$
Up-regulation capacity for early auction in hour t	C_t^{up}	$\forall t \in \mathcal{T}$
Down-regulation capacity for early auction in hour t	C_t^{down}	$\forall t \in \mathcal{T}$
Remaining up-regulation capacity for the late auction in hour t	C_t^{up-rem}	$\forall t \in \mathcal{T}$
Remaining down-regulation capacity for the late auction in hour t	$C_t^{down-rem}$	$\forall t \in \mathcal{T}$
Load predictions with a forecast horizon of 48 hours in hour t	P_t^{pred48}	$\forall t \in \mathcal{T}$
Load predictions with a forecast horizon of 24 hours in hour t	P_t^{pred24}	$\forall t \in \mathcal{T}$
Load predictions with a forecast horizon of 2 hours in hour t	P_t^{pred2}	$\forall t \in \mathcal{T}$
Real load in hour t	P_t^{Load}	$\forall t \in \mathcal{T}$
Number of connected vehicles in hour t	$n_t^{connected}$	$\forall t \in \mathcal{T}$
Demand of FCR-D up in early auction in hour t	D_t^{up-e}	$\forall t \in \mathcal{T}$
Demand of FCR-D up in late auction in hour t	D_t^{up-l}	$\forall t \in \mathcal{T}$
Demand of FCR-D down in early auction in hour t	D_t^{down-e}	$\forall t \in \mathcal{T}$
Demand of FCR-D down in late auction in hour t	D_t^{down-l}	$\forall t \in \mathcal{T}$
Preliminary demand of FFR in hour t based on two day ahead forecast by Energinet t	D_t^{FFR-d2}	$\forall t \in \mathcal{T}$
Binding demand of FFR in hour t based on day ahead forecast by Energinet t	D_t^{FFR-d1}	$\forall t \in \mathcal{T}$
Big M	M	

Table 1: Nomenclature for Decision Models

Acronyms

AEM	Alert State Energy Management
AI	Artificial Intelligence
aFRR	automatic Frequency Restoration Reserve
API	Application Programming Interface
BESS	Battery Electric Storage System
CE	Continental Europe
CO_2	Carbon Dioxide
CPO	Charging Point Operator
CSO	Charging Site Operator
DK2	Electricity Prize Zone in Eastern Denmark
DTU	Technical University of Denmark
EMS	Energy Management System
ENTSO-E	European Network of Transmission System Operators for Electricity
EV	Electric Vehicle
FCR-D	Frequency Containment Reserve for Disturbances
FCR-N	Frequency Containment Reserve for Normal Operation
FFR	Fast Frequency Response
HVDC	High-Voltage Direct Current
ICE	Internal Combustion Engine
LER	Limited Energy Reservoir
MAE	Mean Absolute Error
mFRR	manual Frequency Restoration Reserve
NEM	Normal State Energy Management
R^2	Coefficient of Determination
RMSE	Root Mean Square Error
SE1-4	Electricity Price Zones in Sweden
SOC	State of Charge
TSO	Transmission System Operator
V2X	Vehicle-to-Everything

1 Introduction

According to the United Nations, climate change is the single biggest threat modern humans have ever faced [1]. The main driver for the increase of the average global temperature is the emission of greenhouse gases. In 2021, the largest contributor to Denmark's CO_2 emissions was the transportation sector with 40.6% of the total emissions [2]. To mitigate those emissions, it is the strategy of the country to widely roll out electric vehicles (EVs) and replace internal combustion engine (ICE) vehicles with electric ones, as they provide a way of avoiding local exhaust emissions. Together with the uptake of emission free electricity generation through renewable energy sources such as wind power, there is a strong synergy between the technologies, resulting in a significant reduction of carbon emissions. Even though the argument that EVs are only as clean as the electricity mix fuelling them is often brought up, already with the current electricity mix of the EU, the carbon intensity of EVs is significantly lower compared to ICE vehicles [3]. Therefore, as a part of the European Green Deal, it is the ambition of Denmark to have at least 1 million zero-emission cars on the streets in 2030, which corresponds to a five-fold increase compared to today [4]. Moreover, the electricity generation is reinforced with additional wind power projects. Thus, by 2030 it is the target of Denmark to quadruple the onshore wind power and solar photovoltaic capacity, while offshore wind is expected to reach 18 GW [5].

Yet, the large-scale integration of these technologies causes the electric power system to face serious challenges. An overall increase of electricity demand due to replacement of oil with electricity, higher peak consumption due to high coincidence, as well as matching the charging processes to the fluctuating power generation are critical challenges to be addressed. Uncontrolled charging may overload the distribution grid, which was initially not designed for the inclusion of electric cars [6, 7]. Thus, the network companies are forced to reinforce the grid resulting in high costs, on top of the already existing challenges of replacing aging assets that were often built decades ago [8]. The high costs can be reduced if the charging processes are handled in a coordinated way. Therefore, in various previous work, smart charging strategies are studied and assessed. Vehicle-to-Everything (V2X) services, as classified in [9], can be used for a smoother integration of EVs in the power sector. This can be achieved by providing flexibility throughout the charging process. This flexibility of increasing or reducing charging power can be used for various purposes. For example by providing frequency services, EVs can actively participate in the task of balancing the power grids frequency. According to [10], the demand for balancing services is expected to increase in the future, due to higher shares of intermittent electricity generation. However, it should not be forgotten that the primary use of electric vehicles is transportation. Thus, the users convenience needs to be kept high for a successful roll-out of EVs. Consequently, it is important to leave the freedom of charging times and locations to the user. As a result, the charging processes are coupled to a high extend of uncertainty, making it difficult to effectively use the resource.

The following research questions arise from this setup:

- How can the uncertainty in charging patterns of EVs be overcome?
- Given a prediction of EV charging patterns, how to allocate the resources to ancillary services?
- Is it profitable for EVs to participate in ancillary services?

Therefore, this thesis aims to overcome the uncertainty with a machine learning-based prediction model that aims to forecast charging patterns of EVs at a charging location. For this, real-world data from a workplace parking lot with 12 charging spots on the university campus of the Technical University of Denmark in Lyngby is used. With the prediction of charging patterns, the available amount of capacity for flexibility services is assessed. Additionally, a decision model for the participation in ancillary services is built. The aim of the model is to make an optimal decision for participating in ancillary service markets, more specifically frequency services. This includes a decision whether to participate or not and which service to offer to which extent. Finally, the profitability from those services is estimated.

The remainder of the thesis is organised as follows: In chapter 2, a comprehensive literature review of ancillary services, V2X and machine learning tools for energy applications is conducted. Chapter 3 reviews ancillary services in the Nordic power system, and conducts a thorough market analysis. In chapter 4, the methodology used in this thesis is explained. This includes the design of a machine learning model for load forecasting, as well as a decision model based on linear programming. Chapter 5 presents the real-world case used for the scope of the study. The results of the thesis are shown in Chapter 6, while chapter 7 concludes the work and provides room for discussion.

2 Literature review

Ancillary Services
Ancillary services in the Nordic power system represent a highly relevant and timely research topic, particularly in light of the significant transitions and changes the services are undergoing. A report from the Danish transmission system operator (TSO) Energinet states, that the transition of energy systems to 100% renewable energy introduces new phenomena and characteristics, that require innovative solutions to maintain stable power system operation [10]. The report gives a thorough insight to current markets for ancillary services as well as to expected future developments. Some new concepts that are explained in the report are the Nordic aFRR capacity market, as well as a new Danish national mFRR capacity market. The current market structure of frequency containment reserve is explained, and technologies for the services are analysed. Moreover, a timeline of future expected market changes is given. Energinet foresees a large increase in capacity needed for ancillary services, due to the growth of fluctuating resources such as wind and solar photovoltaic.

Various research articles examine the potential of battery electric storage systems (BESS) to participate in ancillary service markets. In [11], the authors formulate a mathematical model with optimal bidding strategy for batteries in the Nordics. The model is based on a two-stage stochastic mixed-integer linear optimisation, and the focus of the study is on FCR-N, FCR-D and FFR. In [12], the business value of BESS participating in ancillary services is investigated. By considering historic prices of ancillary services, and determining patterns and trends, the authors identify profitable bidding hours. The study helps BESS owners develop a long-term business plan. Thingvad et al. [13] analyse the potential of BESS to participate in ancillary services on top of energy arbitrage. The study considers energy the energy throughput of the battery that occurs due to the participation in the ancillary services, as well as electricity tariffs, and finds an optimal schedule for services to perform in.

Ancillary Service Provision by EVs
Electric vehicles can offer numerous services due to their capability as mobile energy storage units. In [9], the authors detail various flexibility services that EVs can provide, leveraging their potential as batteries on wheels. The authors refer to the concept as vehicle-to-everything, or V2X. The term can further be divided into vehicle-to-grid, home, building or load. Moreover, in [14], ancillary services for electric vehicles are classified into 8 frequency and 32 flexibility services. Additionally, the study takes the perspective from various stakeholders, such as the end-user, the aggregator, the charging-site-operator (CSO), the charging-point-operator (CPO), and both distribution and transmission system operators.

Different business cases for flexibility services of EVs are examined in [15]. Here, the authors investigate the technical and economic feasibility of V2X services, using both residential users vehicles as well as fleet vehicles using a linear programming optimisation. The work in [16] investigates the impact of smart charging on charging costs as well as on CO_2 emissions, comparing a de-centralised and centralised optimisation approach for a parking lot with 12 outlets.

In [17], the focus is put on optimal participation in frequency markets with an aggregation of electric vehicles, while accounting for network constraints. The work in [18] and [19] investigates the potential of an aggregation of EVs to participate in frequency containment reserve for disturbance operation in the early auction. For this, charging patterns of residential users are analysed and used in an aggregation. An optimisation program is formulated that offers capacities according to an availability of at least 90%, as Energinet demands.

The EV4EU project aims to research and implement bottom-up and user-centric V2X management strategies, facilitating the mass deployment of carbon-free transportation. The solutions are applied and tested in Denmark, Greece, Portugal, and Slovenia, with a specific focus on demonstrating services provided by electric vehicles (EVs).

Similarly, the FLOW project (**F**lexible energy systems **L**everaging the **O**ptimal integration of EVs deployment **W**ave) focuses on user-centric V2X smart charging strategies. These strategies are tested, validated, and enhanced in five demonstration sites across the Czech Republic, Ireland, Italy, Denmark, and Spain.

Artificial Intelligence for Energy Applications
Artificial intelligence (AI) is rapidly growing in importance and is increasingly influencing various sectors, including energy applications. [20] makes use of a machine learning approach to optimise the economic profitability of a residential users energy management system. The study uses gradient-boosted decision trees for forecasting, and highlights the trade-offs between model accuracy and complexity, resulting in higher computational time. [21] makes use of deep learning techniques to forecast electric vehicle charging load in Spain, considering seasonality effects.

Contribution
his thesis aims to contribute to both projects by combining electric vehicle load forecasting with the optimal allocation of forecasted capacities to ancillary services in the Nordic power system. Additionally, it thoroughly investigates the current market structure and behavior, examining the suitability of market design. By focusing on the Danish demonstration of flexibility services with EVs, this research not only supports the objectives of the EV4EU and FLOW projects but also provides valuable insights into the practical deployment and management of EV services.

3 Ancillary Services in the Nordics

The following chapter introduces ancillary services in the Nordic power system. In section 3.1,the chapter starts by explaining the need for ancillary services. Moreover, the different services are described and requirements for each service are summarised. In section 3.2, a thorough market analysis of ancillary services in the Nordics is conducted, highlighting patterns and trends and relationships to the electricity spot market. The analysis finds a way to model the prices that can be expected for FCR-D and FFR participation.

3.1 Description of Services

It is crucial for power system operation to maintain the nominal frequency. Various components integrated in the system require the frequency of 50 Hz. In reality, the frequency of the power system constantly hovers around 50Hz with slight deviations. To to maintain the desired frequency, the power drawn and fed into the grid needs to be balanced within a certain band at all times. This is based on the swing equation, as shown in Equation 3.1:

$$P_m - P_e = 2H \cdot \frac{d\omega_m}{dt} \tag{3.1}$$

In this equation, P_m refers to the sum of all power generation in the system, while P_e indicates the sum of all electrical loads. H is the inertia time constant, which is a normalised way of expressing system inertia. The rotational speed ω_m is the rotational speed of the system, which can be expressed as a frequency when considering $\omega = 2 \cdot \pi \cdot f$. From the differential equation, it can be seen that as long as the active power generation and demand are balanced, the frequency remains constant. However, due the the large amount of users connected to the power system that behave independently, this is practically impossible as their demand is uncertain and needs to be forecasted. Moreover, this applies to generation as well, where some generation units have scheduled power output, while others are dependent on environmental conditions such as wind or sun, which need to be forecasted. Additionally, there is always the possibility for unexpected outages or failures of components in the system, which might bring an imbalance. Therefore, there is a need for ancillary services.

There are various types of ancillary services, however, in the scope of this thesis the focus lies on frequency services. Frequency services describe the action of adjusting power, based on the frequency. According to ENTSO-E, frequency services can be distinguished into primary frequency control, secondary frequency control and tertiary frequency control [22]. The goal of the primary frequency control is to stabilise frequency and reduce the rate of change of the frequency, in a time frame of seconds. The secondary frequency control aims to restore the frequency back to the nominal value, while the tertiary frequency control aims to relieve the secondary control in a time frame of minutes to hours. In the Nordic power system, the distinction between frequency services is more granular. Faster services, such as Fast Frequency Response (FFR), Frequency Containment Reserve for Disturbance (FCR-D), Frequency Containment Reserve for Normal Operation (FCR-N) can be categorised as primary frequency control, while automatic Frequency Restoration Reserve (aFRR) and manual Frequency Restoration Reserve (mFRR) represent secondary and tertiary frequency control respectively. The need for the faster reserves can be explained when comparing the frequency of the Nordic synchronous area with the one of Continental Europe (CE).

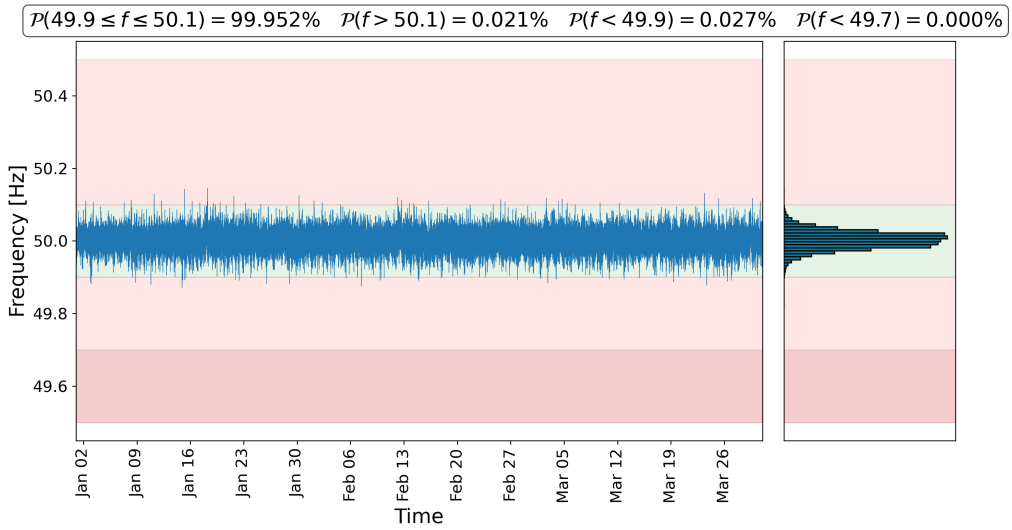

(a) Continental Europe

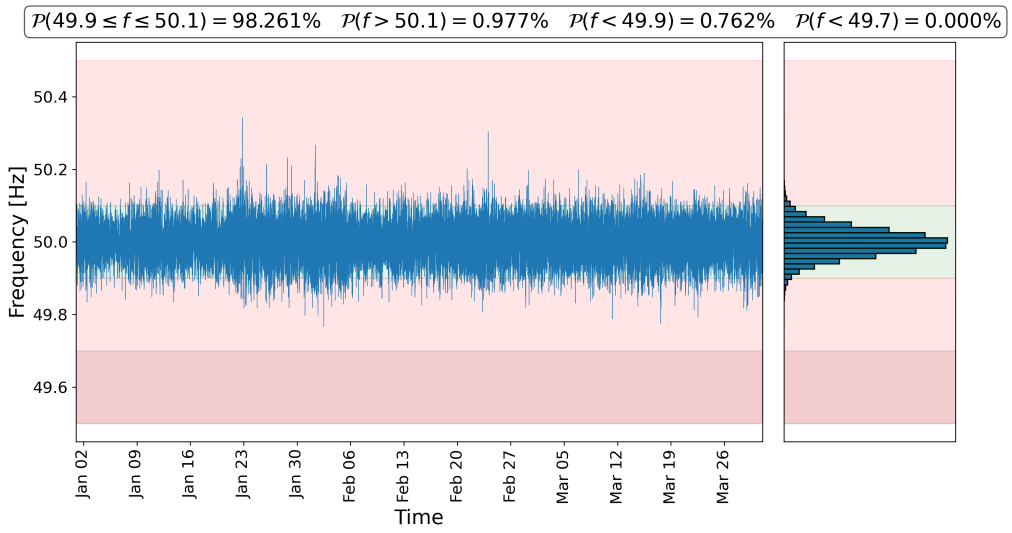

(b) Nordics

Figure 3.1: Frequency over time in the Nordic and CE synchronous area

Figure 3.1 shows the frequency timeseries of the power system from January to March 2024, and a histogram of the frequency [23, 24]. The coloured backgrounds represent zones in which FCR-N, FCR-D and FFR are activated, which are described afterwards. It is evident that the frequency of the Nordic system fluctuates significantly more than that of the CE system. Additionally, the probability $\mathcal{P}$ shows the likelihood of the frequency in a certain zone. Therefore, it can be seen that the frequency of the continental system is outside of 49.9 and 50.1 Hz only 0.021% and 0.027% of the time. On the other hand, in

the Nordic system, these numbers increase to 0.977% and 0.762%.

This behaviour can be explained by considering Equation 3.1. Due to the smaller system size and large-scale rollout of fluctuating renewable energy resulting in smaller system inertia, the frequency is exposed to a more drastic rate of change in case of an imbalance. In return, this calls for a faster response by the frequency services. The frequency services in the Nordic power system are shared proportionally to their demand share by the four countries Denmark, Sweden, Norway and Finland The following subsections explain the established frequency services in the Nordics, in order of response time:

3.1.1 FCR-N

Frequency containment reserve for normal operation is an automatic regulation provided by generation and demand units, adjusting the power setpoint based on the frequency. The frequency service must be supplied linearly in a range of ±100 mHz, corresponding to an operating range from 49.9 Hz to 50.1 Hz [25] without a deadband. For frequencies outside of the range, the service remains fully activated. Considering this operating range and comparing to Figure 3.1b, it can be seen that FCR-N is activated partially 98.26% of the time, while the remainder of the time it is fully activated.
FCR-N is a symmetrical service, which means that a unit or portfolio supplying the service needs to be able to both increase and decrease the power setpoint, based on the frequency. Therefore, the provider needs to supply upwards and downwards regulation, in under- and overfrequency situations respectively. The activation of FCR-N follows a droop implementation, where the full capacity is activated at 100 mHz deviation from 50 Hz. The response between is implemented linearly, as seen in Figure 3.2. The figure additionally shows the allowed operating range, which corresponds to an overshoot and undershoot of 5% and 10% respectively. In terms of response time, the maximum delay of 2.5 seconds is allowed

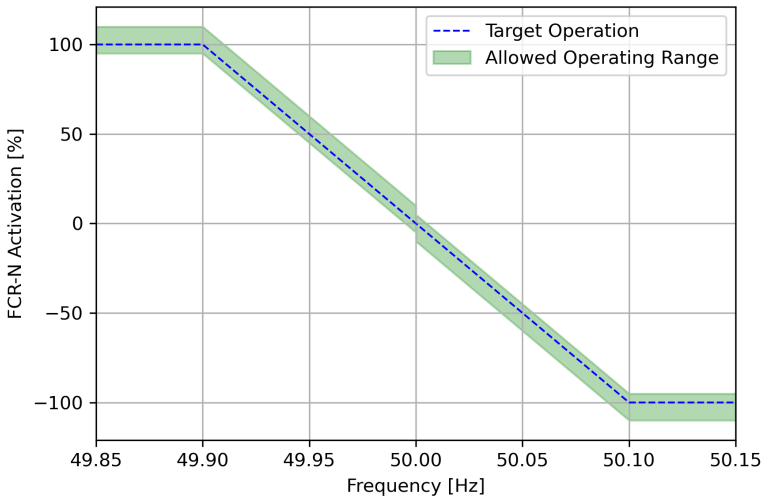

Figure 3.2: FCR-N droop

as a start-up time. Additionally, the reserve must be able to supply 63% within 60 seconds and 95% within 180 seconds.

Further regulation applies to units that are considered as limited energy reservoirs (LER). Units are classified as LER, if they can not sustain a full FCR-N response in both directions for 2 consecutive hours, without including additional charging/discharging strategies. Due to the symmetrical characteristic of FCR-N, therefore a unit is classified as LER if it

can not endure a maximum of 4 hours of activation. Aggregated portfolios are considered a LER, in case that the entire portfolio together can not fulfil the activation time constraints. Therefore, portfolios including batteries that would be considered LER if they were alone, do not necessarily have to be considered LER. LER units or portfolios must implement an energy management system (EMS), for which both power and energy needs to be reserved. The EMS needs to consist of one system for normal state (NEM) and one for alert state (AEM). The unit/portfolio needs to reserve 34% of the prequalified FCR-N power in both directions, as well as 1 hour of full FCR-N activation as energy. This means, that if a unit wants to offer 1 MW of FCR-N, it needs a to be able to increase and decrease the power by at least 1.34 MW. Additionally, it must reserve 1 MWh of stored energy as well as leave room to charge 1 MWh.

FCR-N is procured by the Danish TSO Energinet in collaboration with the Swedish TSO Svenska Kraftnät, in the form of a combined auction to maximise market efficiency. The combined hourly volume is determined once per year, for 2023, this combined volume was 258 MW. The necessary volume is auctioned on the day before the operation (D-1), where a part of the volume is auctioned in an early auction at 00:30 (D-1 early), while the remaining required volume is purchased in a late auction at 18:00 (D-1 late). Suppliers submit hourly offers for the coming day, and additionally have the opportunity to offer block bids. In the D-1 early auction, a block bid is allowed to have a maximum duration of 6 hours, while in the late auction a block bid is allowed to have a duration of up to three hours. Suppliers shall submit their offers as an hourly volume in MW and an hour-by-hour price in €/MW or DKK/MW. In the case that a bid is entered with a price in DKK/MW, Energinet converts the bid into €/MW before it will be redirected to Svenska Kraftnät. Bids have to be submitted with a minimum volume of 0.1 MW with possible increments of 0.1 MW. All bids are always either accepted in their entirety or not at all, meaning that no bids are partially accepted. Both D-1 early and D-1 late auctions are cleared separately.

All accepted bids are remunerated with a reserve payment, based on the reserve price, which is equal to the highest accepted bid in €/MW, according to the marginal price or clearing price principle. However, due to the possibility of offering block bids, cases might occur in which a bid with an offering price below the marginal price is not selected. This is because the TSOs clear the market in a way that covers the required volume and incurs the least overall cost. In addition to the reserve payment, suppliers also receive an energy payment. The energy payment is composed of a payment for upwards regulation and a payment for downwards regulation. The payment for upwards regulation is based on the upwards regulation price, while the payment for downwards regulation is based on the downwards regulation price respectively.

The correct activation according to the frequency is controlled ex-post, after the day of operation. If Energinet detects, that a supplier could not follow the control signals and thus could not deliver the contracted amount of FCR-N, a penalty is issued. In this case, the payment made to the supplier is reduced proportionally to the time that the service was delivered correctly. Further compensation might be demanded by Energinet, that are based on the additional costs that arose due to the non-delivery. Additionally, if it is detected that a supplier frequently can not deliver the agreed service, he might be excluded from the market, as discussed in [26].

3.1.2 FCR-D

In contrast to FCR-N, FCR-D is not a symmetrical product. This means, that the upward and downward regulation is split into two unique products: FCR-D up and FCR-D down.

Both FCR-D services are automatic regulation that can be supplied both by generation units as well as demands, that can adjust their power setpoint as a function of the system frequency. FCR-D up is a fast service that is activated in underfrequency situations, starting from 49.9 Hz. On the other hand, FCR-D down is an overfrequency service which is activated starting from 50.1 Hz. The split between the two services is shown in Figure 3.3.

Corresponding to Figure 3.1b, FCR-D up and FCR-D down are activated 0.762% and

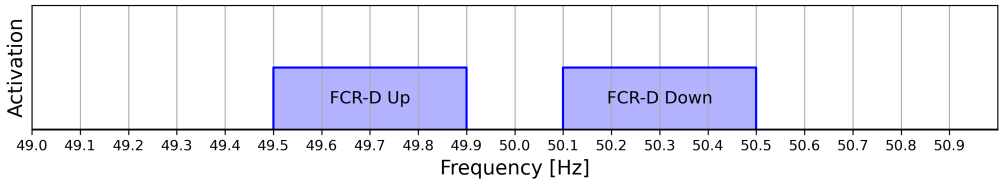

Figure 3.3: FCR-D split

0.977% of the time. Additionally to the split in upwards and downwards regulation, both FCR-D services are also split into dynamic and static. In this regard, the dynamic means that the supplier is able to follow a droop implementation, while the static service is especially suited for technologies that can not adjust their power output based on a droop. Figure 3.4 provides an overview of the target response of FCR-D and allowed operating ranges. The target response shows the deadband which goes ±100 mHz in both directions around the nominal frequency of 50 Hz. Then, from the starting point of the operation at 49.9 Hz and 50.1 Hz until the maximum activation at 49.5 Hz and 50.5 Hz respectively, the activation increases linearly. For both FCR-D services, the maximum allowable deviation from the target operation is 5% in the case of under-delivery and 20% for over-delivery.

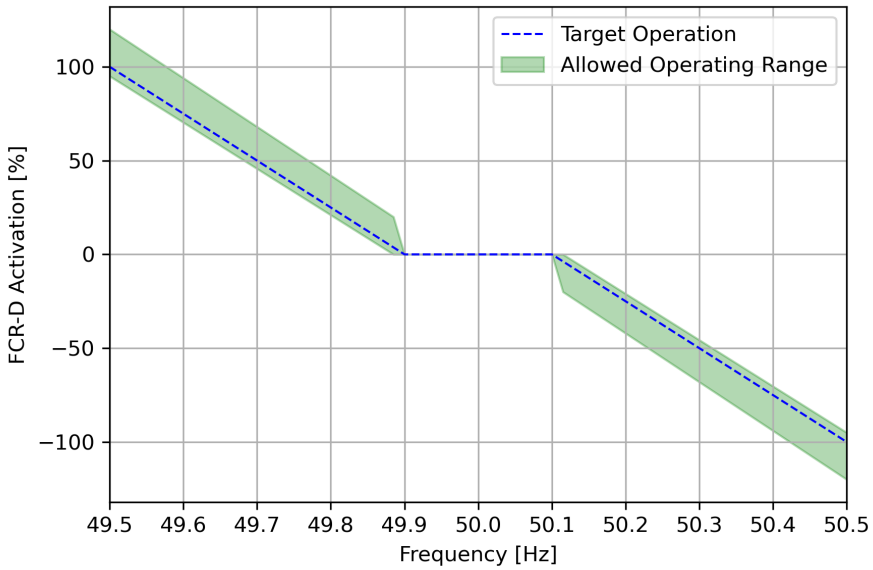

Figure 3.4: FCR-D dynamic range

Additionally, several ramping constraints apply to both FCR-D services. The supplying unit must deliver a response within 2.5 s and must be able to supply 86% of the response

within 7.5 seconds. Moreover, the unit must be able to ramp in a way that supplies energy equal to 3.2 seconds times the reserved power within 7.5 seconds.

Moreover, there are additional rules for LER units/portfolios. Again, units/portfolios are classified as LER in case that they can not provide a continuous full FCR-D provision for at least 2 hours without implementing additional charging or discharging strategies. Since FCR-D is asymmetrical, a unit needs to be able to deliver 2 hours of full activation if it only bids in one direction, while it needs to be able to deliver full activation for 4 hours if it bids for both FCR-D up and FCR-D down. LER units/portfolios need to reserve 20% of the prequalified FCR-D amount in the opposite direction, as well as reserve energy corresponding to 20 minutes of full activation. This means, that a unit that wants to offer 1 MW of FCR-D up, needs to reserve 0.2 MW of FCR-D down capacity, as well as 0.33 MWh of energy according to 20 minute activation.

FCR-D is procured in shared market between Denmark and Sweden. The required volume for the whole Nordic power system is determined by the dimensioning fault, which is equal to the largest possible single fault (N-1) in the Nordics. According to Energinet, the largest possible fault is 1.4 GW, which corresponds to the largest nuclear power station in operation [27]. However, it is up for debate if this number corresponds to the largest possible fault, as the tripping of the Finnish Olkiluoto 3 lead to a 1.6 GW failure[28]. Additionally, the introduction of the Nordlink high-voltage direct current (HVDC) interconnector that connects Germany and Norway with a capacity of 1.4 GW raises concerns, as there is the opportunity to switch from export to import and the other way around, resulting in a possible maximum imbalance of 2.8 GW [29].

The share for Denmark and Sweden is determined proportionally to the demand share, where in 2023 the requirement for FCR-D up has been 44 MW for Denmark and 580 MW for Sweden, resulting in a total of 624 MW. The requirement for FCR-D down has increased gradually over the last years, where the combined requirement for Denmark and Sweden was 318 MW in Q3 2023, 363 MW in Q4 2023, 408 MW in Q1 2024 and 453 MW in Q2 2024. Svenska Kraftnät expect that the full volume requirement will be reached by 2025. Therefore, the volume for the combined Danish-Swedish auction is 624 MW.
The volume for both FCR-D up and down is procured via two auctions on the day before the operation, on D-1 early and D-1 late. Here, a part of the required volume is auctioned in D-1 early, and the remaining required volume is auctioned in the D-1 late auction. Previously, the price was paid out according to a pay-as-bid principle, however since February 2024 the marginal price principle is applied The minimum bid size for FCR-D is 0.1 MW, with increments of 0.1 MW.

3.1.3 FFR

Fast Frequency Response is the fastest frequency service in the Nordics. FFR is activated automatically in underfrequency situations as a response to major disturbances from generation units or power lines in low-inertia situations. There are three options for activation frequency of FFR: a) 49.7 Hz, b) 49.6 Hz and c) 49.5 Hz, which can be freely chosen by the provider. Depending on the selected activation frequency, the response time of the service varies. In case a), the slowest response time is demanded, where a the full power needs to be activated in a maximum of 1.3 seconds. For case b) and c) the maximum time for full activation is 1.0 and 0.7 seconds respectively. The alternatives are visualised in Table 3.1. In addition to the three options for activation frequency and response time, there are two options for the duration of the full activation, namely long and short. For alternative 1), the activated power must be kept up for at least 5 seconds, after which the deactivation is

Option	Activation frequency [Hz]	Maximum full activation time [s]
a)	49.7	1.3
b)	49.6	1.0
c)	49.5	0.7

Table 3.1: FFR options

allowed to be carried out with a maximum gradient of 20% per second, and must be fully deactivated within 30s after the disturbance. After the full deactivation, the unit must hold the operating point for at least 10s . This means, that e.g. a battery injecting power to the grid is not allowed to "recharge" directly after the deactivation as a rebound, but has to wait 10 seconds.

With alternative 2), the activation must remain longer, namely for 30 seconds. After the 30 seconds however, there are no requirements and the deactivation can be carried out immediately. For both alternatives, the reserve must be fully available again 15 minutes after the disturbance. Additionally, for both alternatives and all three options, the maximum rebound after the deactivation is 25% of the contracted capacity. Moreover, the maximum overshoot during the injection is 35% of the contracted power. As a result, the following allowed responses are given in Figure 3.5.

In Figure 3.5a, the short connection remain is described. The figure shows the response to a disturbance at t_0, after which it can be observed that the service is activated fully within 1.3 seconds at t_1, whereafter the activation remains for 5 seconds until t_2. Then, the deactivation process begins and the power is reduced with the maximum allowed gradient of 20% per second, resulting in a complete deactivation after 5 further seconds at t_3. The asset then needs to hold this operating point for 10 seconds, before it is allowed to rebound at t_4. At t_5, the service needs to be fully deactivated.
For the long activation, the ranges are shown in Figure 3.5b. It can be seen that again, the service is fully activated 1.3 seconds after the disturbance at t_0. From the full activation at t_1, the power needs to be kept up for at least 30s, until t_3 from where it is allowed to deactivate without further requirements.

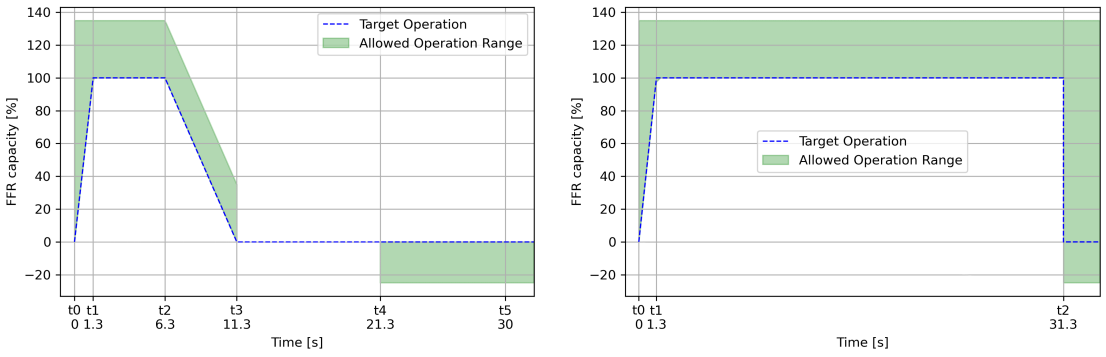

(a) Alternative 1) short

(b) Alternative 2) long

Figure 3.5: FFR response for option a)

The demand for FFR is mostly seasonal, due to generally lower system inertia as a result from larger renewable energy share in the summer months from May to September. In the winter months from October to April, FFR is mostly non-existent, with exceptions around the winter holidays.

The supply of FFR is auctioned daily for every hour of the next day in a Danish national auction, which is held at 15:00. Participants must express their offers as an hour-by-hour volume and price. The minimum volume is 0.3 MW, with increments of 0.1 MW. The offering price needs to be expressed in DKK/MW/h or €/MW/h, with two decimal points. The hourly demand of FFR is continuously forecasted every day for the next seven days by the Danish Transmission System Operator (TSO) Energinet [30] and is published daily at 10:00. The forecasted volume one day ahead becomes binding and is used as the auction volume. All accepted bids receive an availability payment in accordance to the clearing-price, the highest accepted bid.

3.1.4 Prequalification of non-controllable units or portfolios

Energinet considers that there are significant differences between conventional units and non-controllable fluctuating resources. The distrinction between centrally controlled units and not-centrally controlled units, is according to the following characteristics: One one hand, centrally controlled units are dispatchable, their baseline power is rooted, and the units baseline has no external affections besides from outages. On the other hand, non-centrally controlled units are non-dispatchable, their baseline is dependent on external affections such as weather or end-user behaviour.
The crucial differences regarding the participation in ancillary service markets are a) the certainty of availability, as well as b) the baseline power.

(a) A fluctuating unit/portfolio can not guarantee at the time of the bidding (D-1) that the capacity is truly available

(b) A fluctuating unit/portfolio might experience changes in power output/consumption, that are not related to the frequency control

Still, the participation in the ancillary service markets is achieved via the participation in the markets before the day of operation. Therefore, Energinet offers a different approach for the offering strategy and the verification of correct participation. The calculation of available capacity for the following day is regarded as an "ex ante" forecast, while the baseline is determined as an "ex-post" estimation. Energinet offers an incentive for not-centrally controlled units, so that they are allowed to offer capacity according to the 10^{th} quantile of a probabilistic forecast, which is referred to as baseline in this study. This ensures, that in 90% of the time, the offered capacity or more is available. This forecast must be based on at least 3 months of data. The reference power, is calculated ex-post to validate the correct response of the ancillary service. The verification is then done according to:

$$Ancillary\ Service\ Response = Actual\ Production - ReferencePower \tag{3.2}$$

Then, the ancillary service response can be compared to how it should have responded according to the offered bid and the frequency. In case that they do not align, the units needs to repay the revenue of the agreed service.

3.1.5 Frequency Services with Electric Vehicles

Traditionally, the generation of power was performed with conventional generators using fossil fuels, that can be scheduled. The demand side, however, remained uncertain and

was forecasted with large amount of historical data. Yet, with more and more fluctuating resources on the generation side, such as wind power and photovoltaic, there is a need to perform frequency services on the demand side. The active power on both generation and demand side can be split into controllable and non-controllable:

$$(P_m^c + P_m^{nc}) - (P_e^c + P_e^{nc}) = 2H \cdot \frac{d\underline{\omega}_m}{dt} \tag{3.3}$$

The charging of electric vehicles can be considered a controllable load, that can adjust the power demand based on the frequency. Not all frequency services however, are suitable for the participation of electric vehicles in a workspace parking lot, as used in this study.

- FCR-N is unsuited because of continuous activation, leading to a disturbance of the charging process. The primary focus of the charging process in the workspace parking lot is the "refuelling" of the battery. To remain user satisfaction high, a substantial increase of state of charge of the battery needs to be ensured, which can not be guaranteed with FCR-N
- aFRR and mFRR are unsuited as well because of long activation times, which disturb the charging process.

Therefore, services that are activated only rarely and for short time periods are preferred. From the previous analysis, it can be seen that FFR is profitable, however only necessary in few hours of the year. Furthermore, FCR-D also provides large profitability margins, and is demanded in larger volumes. *As a result, the study continues to investigate a combination of FFR and FCR-D participation.*

3.2 Market Analysis

This section sheds light on market characteristics, offering insights into price trends and volume fluctuations in FCR-D and FFR markets. Additionally, it identifies significant correlations and dependencies, providing understanding of the factors influencing the different ancillary services.

3.2.1 FCR-D up

Figure 3.6 shows the evolution of the auctioned volumes and prices for FCR-D up from January 2023 until May 2024. It can be seen from the purple line, that the total volume auctioned is not constant, but fluctuates around a mean value of 580 MW. It becomes clear, that the required volume of 624 is not served from sources in DK2, and SE1-SE4. This is because of the way that the Nordic FCR-D market is cleared [31]. Since the FCR-D early auction in Norway has an earlier gate closure time than the one of the combined market for Sweden and Denmark, excess bids from Norway are made available to the Danish-Swedish auction, as well as to Finland. Therefore, the obligation to serve 624 MW is achieved, even though in Figure 3.6 it does not show. Additionally, it can be seen that during the summer months, the volume has a tendency to be served to a higher degree from Sweden and Denmark, while in the winter months a larger share is made available from Norway. Moreover, the hours where the total volume is larger than the demanded 624 MW can be explained by the block bid auction design, where bids are indivisible. It is a possible result of the market clearing mechanism that more than 624 MW are selected, if the overall cost lower when a whole block is accepted.

The green and yellow lines in Figure 3.6 break down the FCR-D up auctions in D-1 early and D-1 late. In the figure, the upper plot shows the FCR-D up volumes that are demanded, while the lower plot shows the prices. It can be seen from the orange lines, that

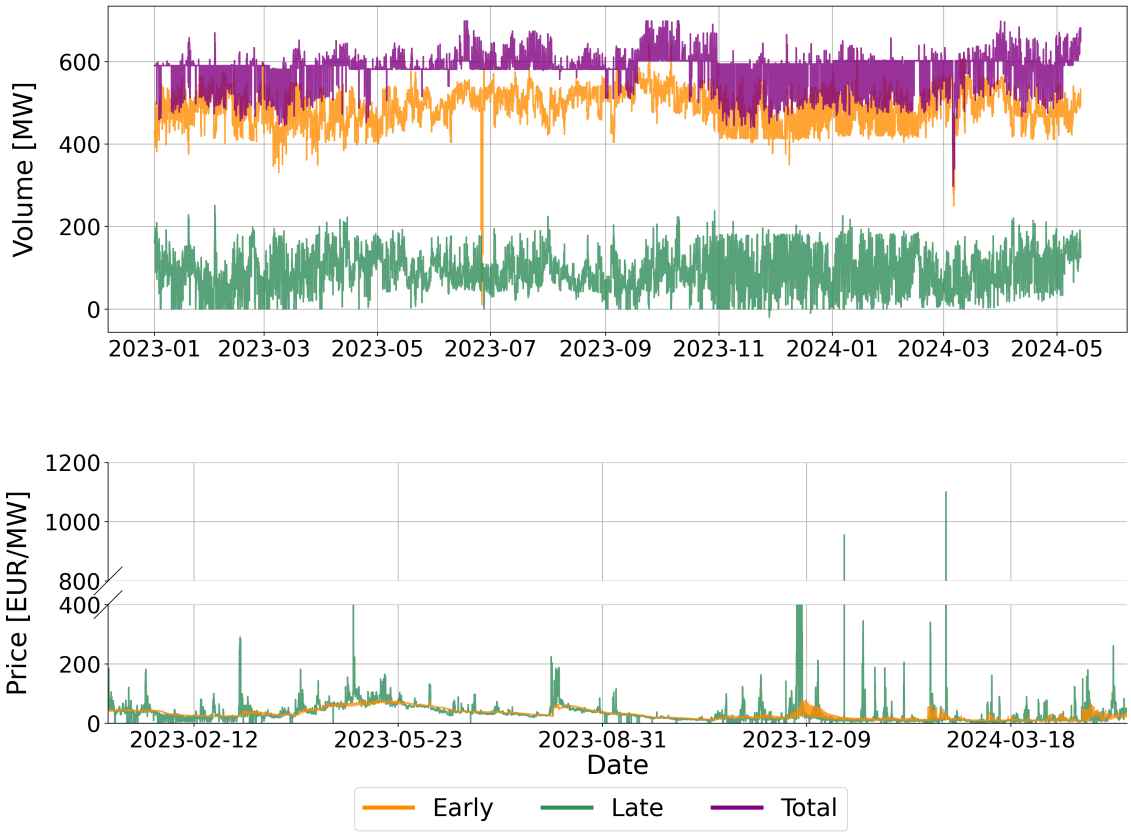

Figure 3.6: Volume and price for FCR-D up

the majority of the volume is auctioned at the early auction, where the volumes are mostly between 450 MW and 530 MW. Also, it can be seen that the prices are stable, with little price fluctuation. For the late auction, shown in green, it is visible that the auctioned volumes are considerably smaller, with most values ranging in between 50 MW and 130 MW. It can also be seen, that for few hours in the considered time period, the volume traded in the late auction is zero, showing that the full required volume was previously purchased in the early auction. Moreover, it can be seen that the prices are less stable, with price spikes that reach up to 1099 €/MW, as indicated with the gap in the y-axis of the subfigure.

Regarding prices, it can be seen that there is an increase in price in the spring of 2023, and more fluctuating prices from November onwards. It can also be seen, that the change from pay-as-bid to marginal pricing in February 2024 brought more noise to the prices. Reason for this, is that before the reported price represents the average accepted bid, while from February 2024 on it shows the clearing price.

Moreover, Figure 3.7 illustrates the autocorrelation of prices for both the early and late FCR-D up auctions. In Figure 3.7a, the autocorrelation of the early auction prices demonstrates a strong dependence on previous prices, with noticeable peaks occurring every 24 hours. This indicates that the price variations within a single day have a tendency to follow consistent patterns - e.g. the price at 13:00 is mostly dependent on the price of 13:00 on the previous day. In contrast, Figure 3.7b shows the autocorrelation for the late auction prices, where the influence of previous prices is significantly weaker, with autocorrelation values around 50% after 24 hours. While there are still peaks every 24 hours, they are less pronounced than those in the early auction.

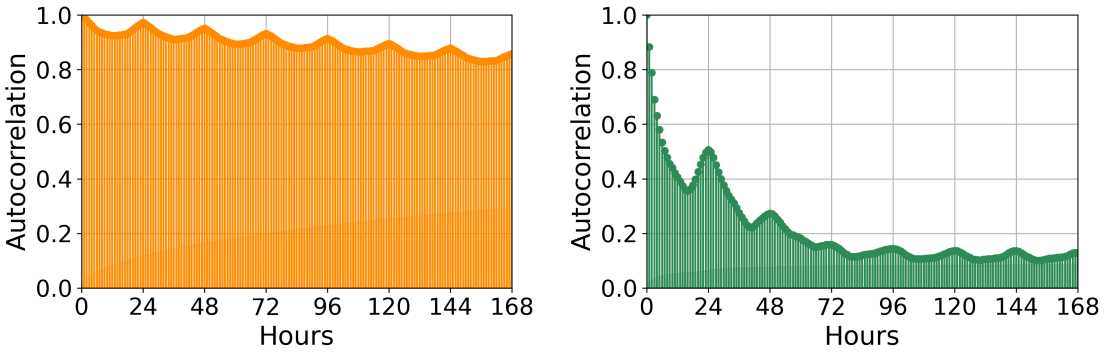

(a) Autocorrelation D-1 early

(b) Autocorrelation D-1 late

Figure 3.7: Autocorrelation of prices for FCR-D up

3.2.2 FCR-D down

For FCR-D down, in Figure 3.8 it can be seen from the purple curve that the total volume continuously increased since the beginning of 2023. It is visible, that the adjustments in demand increases in steps corresponding to the quarters of the year. Again, it can be seen that there are deviations from the precise demand obligation that is to be served, which is explained by the market clearing principle including block bids as well as from the exceeding bids from Norway. It is noticeable however, that there are considerably less negative deviations from the designated value compared to the FCR-D up auction, indicating that there are fewer bids from Norway that are made available to Denmark and Sweden. This shows that FCR-D down is served to a higher degree from Danish and Swedish sources. Additionally, there are fewer deviations in positive direction, indicating that there might be less block bids in the FCR-D down auction compared to the FCR-D up auction. The orange and green curves show the outcome of the FCR-D down market broken down into the early and late auctions. The majority of the volume is auctioned in the early auction, while less demand is covered from the late auction. It can be seen that the volume from the early auction continuously increased over the time, while the late auction has remained more stable in terms of volume. This shows, that the majority of the growth of total demand is covered in the early auction. Another insight is that the volume in the late auction is rarely ever 0 MW, showing that there is rarely an early auction that fully covers the demand.

Regarding prices, it can be seen that the price level for FCR-D down is generally higher compared to the FCR-D up service. It can be seen, that the prices of the early auction are mostly stable, with higher magnitues in the spring and summer months and low prices in winter. However, in spring 2024 after the introduction of the marginal price mechanism, the price levels are also fluctuating stronger than before. The prices of the late auction are subject to severe price spikes and high volatility, with prices reaching up to 10,000 €/MW in spring 2024.

The analysis of the autocorrelation of FCR-D down prices in Figure 3.9 show similar results to the one for FCR-D up. In Figure 3.9a, high influence of previous values in the timeseries can be seen, with noticeable peaks every 24 hours. The late auction in Figure 3.9b shows very low autocorrelation on the other hand, which indicates that the values fluctuate significantly.

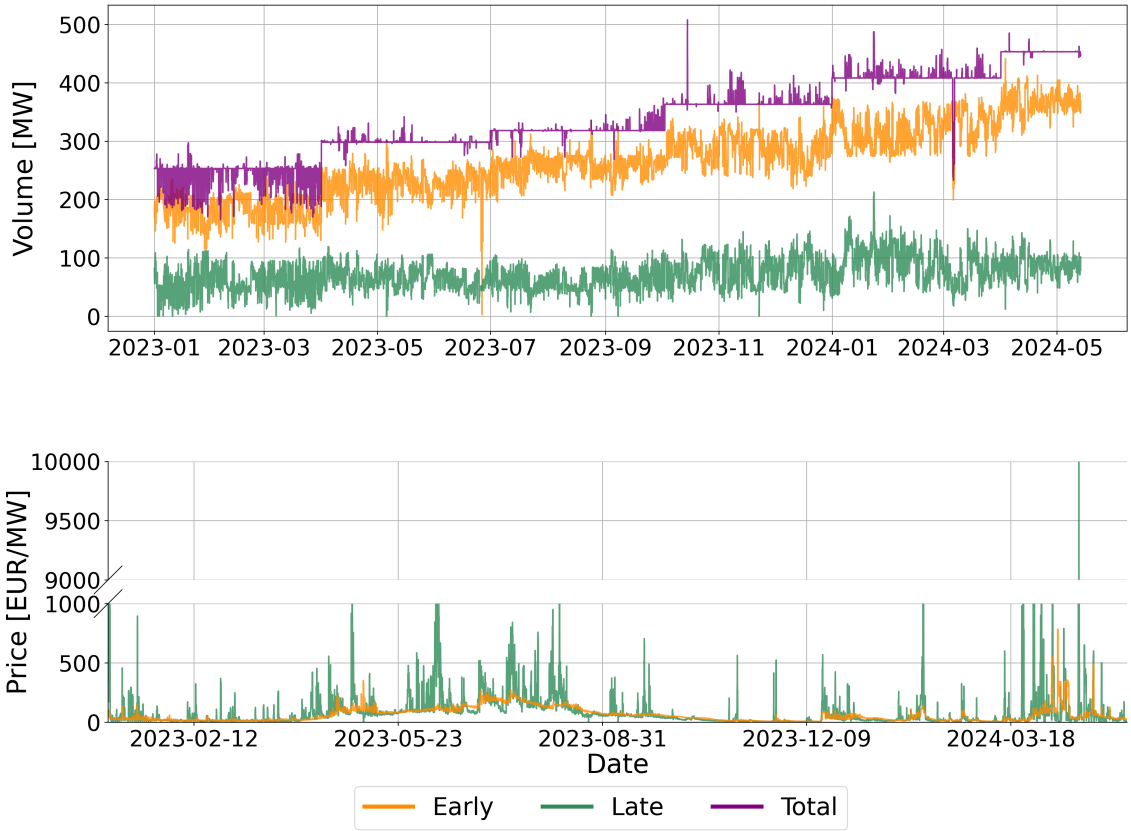

Figure 3.8: Volume and price for FCR-D down

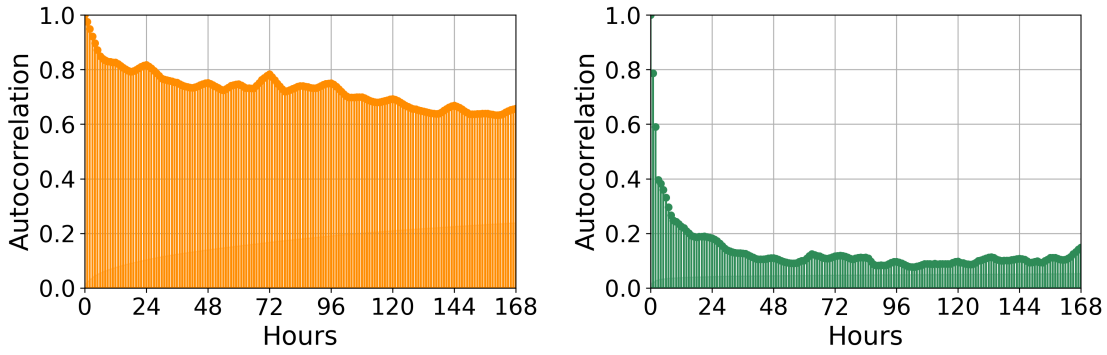

(a) Autocorrelation D-1 early

(b) Autocorrelation D-1 late

Figure 3.9: Autocorrelation of prices for FCR-D down

3.2.3 Relationship of spot prices and FCR-D late auction

Since the autocorrelation of the prices in the late auction for both FCR-D up and down is low, the relationship between the spot electricity price and the outcomes of the late auction is examined. Figure 3.10 shows this relationship for FCR-D up and FCR-D down. It can be seen, that the two services behave inversly in response to the spotprice in DK2. While FCR-D up has low prices when the spot electricity price is low, the price increases in hours with high spotprices. On the other hand, the price for FCR-D down is high when the spot price is low, while the price reduces with increasing spotprices. This effect increases drastically with negative spot prices. For both services, a trendline based on

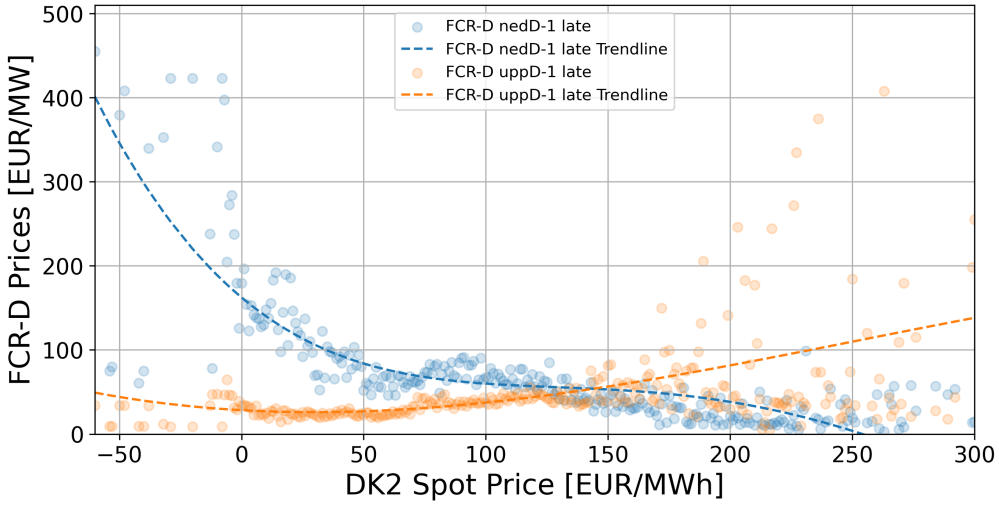

Figure 3.10: Relationship between spot prices and FCR-D prices in the late auction

a 4th-order polynomial has been fitted to the data points. This trendline is assumed to represent the behaviour for spot electricity prices between -50€/MWh and 300€/MWh. For FCR-D up, the polynomial equation is:

$$\lambda_t^{up-l} = -2.586 \cdot 10^{-10} x^4 - 3.666 \cdot 10^{-6} x^3 + 0.002881 x^2 - 0.1612 x + 28.35 \tag{3.4}$$

For FCR-D down, the polynomial equation is:

$$\lambda_t^{down-l} 8.594 \cdot 10^{-8} x^4 - 7.604 \cdot 10^{-5} x^3 + 0.02084 x^2 - 2.435 x + 162.5 \tag{3.5}$$

Where x denotes the spot price in hour t.

The behavior of the price curves can be understood by examining the characteristics of the units providing these services. According to Energinet, the capacities of various technologies are prequalified for participating in FCR-D, as shown in Table 3.2.

For example, a for a flexible **demand** unit, FCR-D up corresponds to a decrease in load, whereas FCR-D down corresponds to an increase in load. When prices are low, there is an incentive to operate at full capacity, leaving little flexibility to increase demand further, thereby resulting in high prices for maintaining that flexibility. Conversely, when prices are high, operating at maximum capacity is less desirable, reducing the flexibility to cut power demand.

Service	Battery	Power Plant	Electric Boiler	Flexible Consumption	Solar PV
FCR-D up	5.0	104.0	3.6	0.5	0.5
FCR-D down	2.1	48.0	2.0	1.7	15.0

Table 3.2: Prequalified capacities for FCR-D up and down by technology [MW]

From the perspective of a flexible **generation** unit, FCR-D up means increasing power output, and FCR-D down means reducing power output. During periods of low electricity spot prices, operating at full capacity is not economically attractive due to low remuneration, limiting the ability to further reduce power output and leading to high prices for FCR-D down. Conversely, when spot prices are high, operating at full capacity is desirable, limiting the ability to increase output further and resulting in high FCR-D up prices.

3.2.4 Fast Frequency Response

The fastest responding primary frequency service, Fast Frequency Response (FFR) is not purchased continually with a fixed volume per hour. Instead, a forecast made by Energinet is used, that determines the necessary amount of FFR demand to ensure safe system operation. The demand of FFR is based on the inertia of the system, which is influenced by the amount of renewable power generation in the system. According to Energinet, FFR is mainly purchased in the summer months starting from May until the end of September. Figure 3.11 shows a heatmap containing the average hourly FFR per month. The analysis of the average demand of FFR by month and hour shows, that in this summer period, FFR is mostly needed during the night and around noon, while in high load periods in the morning and evening, FFR is less demanded. Regarding prices,

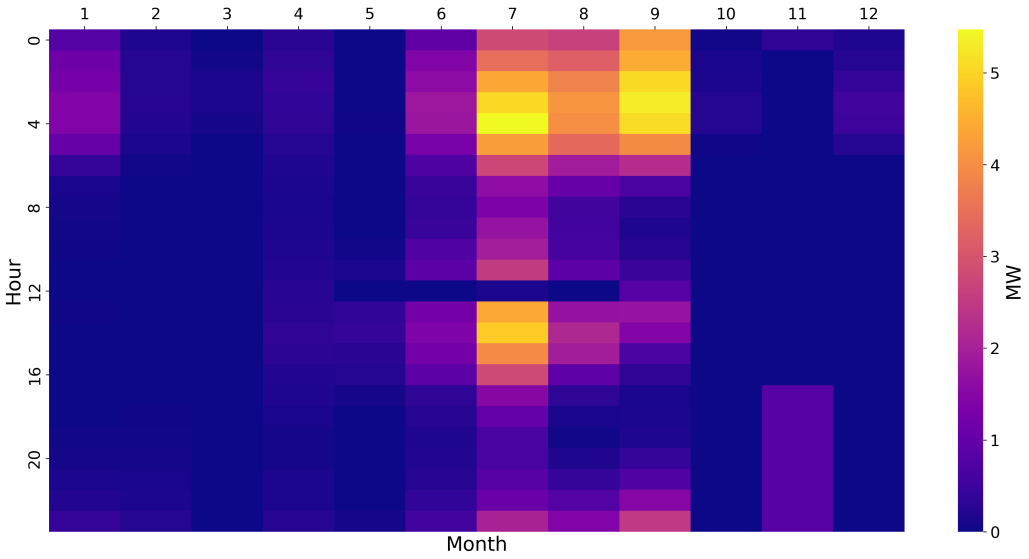

Figure 3.11: Heatmap of average FFR demand per month and hour

Figure 3.12 shows the average price for FFR per month and hour. A comparison between the two heatmaps shows, that to some extend the prices and demanded volumes align. However, it is noticeable that FFR is subject to higher prices in January, even though the

demand is considerably low. Moreover, the demand around noon can be covered with a lower price than the demand in the night.

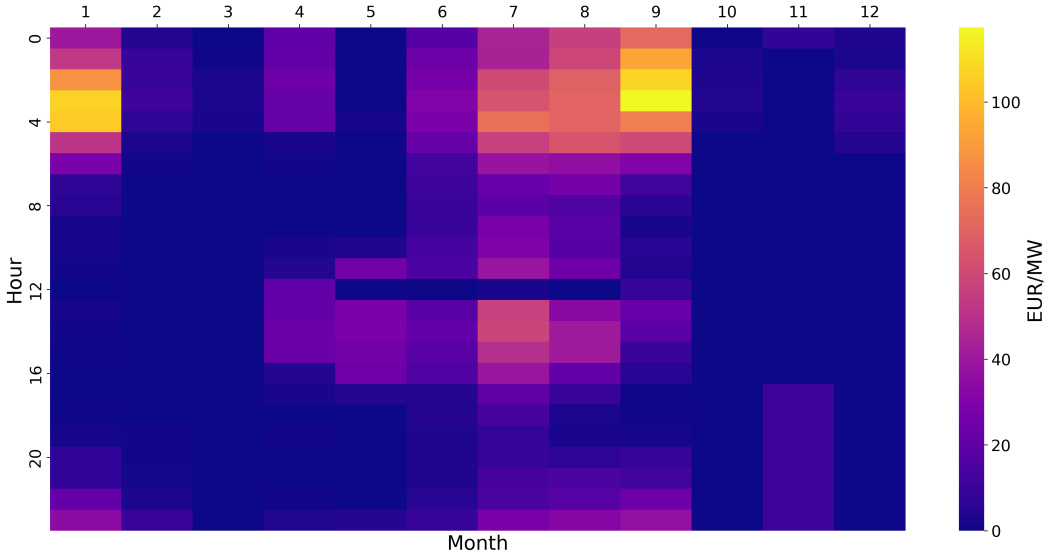

Figure 3.12: Heatmap of average FFR price per month and hour

Since FFR is not purchased continuously, an analysis of the autocorrelation of the prices can not be used to project the prices. Therefore, Figure 3.13 shows the relationship betweeen the price of FFR and the volume purchased. It can be seen, that the price of FFR has a tendency to increase with the demanded volume. Nevertheless, the price reaches a plateau at a volume of roughly 8 MW. However, the majority of purchases of FFR have volumes between 0 and 6 MW. A polynomial has been fitted to the datapoints, showcasing a trendline. The relationship between price and volume of FFR is characterised as:

$$0.0304x^4 - -0.8397x^3 + 5.2811x^2 + 19.8770x + 9.4542$$

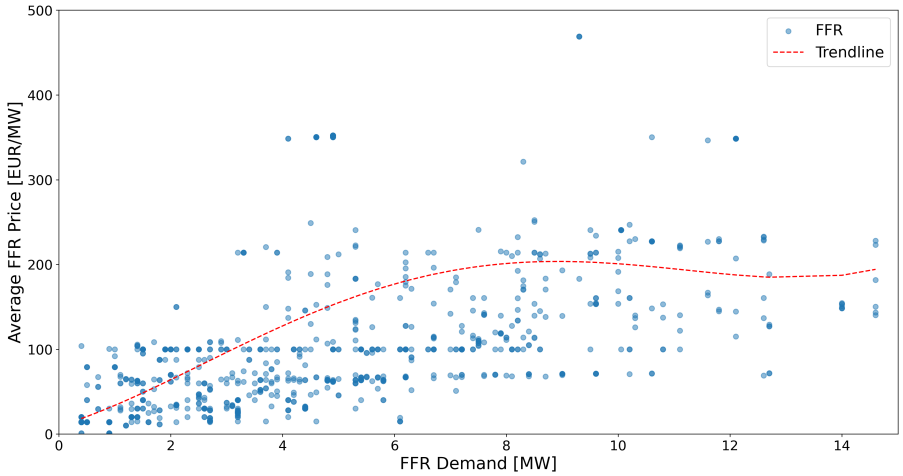

Figure 3.13: Relationship between FFR volume and price

4 Methodology

The following chapter describes the methodology used for the thesis. The chapter is divided into two sections, where the section 4.1 describes the relevant information about the machine learning approach for load forecasting, while in section 4.2 the decision model is described. Generally, two assumptions are important to consider:

- Based on the findings of [32], it is assumed that the chargers in the parking lot are able to adjust their consumption, based on control signals corresponding to the frequency. It is assumed, that the response time is fast enough for the frequency services FCR-D and FFR.
- The constraints to the minimum bid volume and possible increments described in section 3.1 are relaxed, to find the economic value of the available resources. As a result, it is considered to be possible to offer volumes below the minimum bid size of 0.1 MW for FCR-D or 0.3 MW for FFR. Moreover, it is considered to be possible to offer volumes with any increment. The reason for this relaxation is, that an aggregator could add EV parking lots to their portfolio, which already satisfies the minimum bid size. Thus, by relaxing these constraints it is possible to find the true economic potential of EVs participating in frequency services.

4.1 Machine Learning for Load Forecasting

4.1.1 Model Introduction

The following subsections introduce various machine learning algorithms, that are investigated for EV load forecasting. This is formulated as a supervised learning problem, where the value that is to be forecasted is called *label* and the parameters on which the forecast is based on is called *feature*. In the case of the EV load forecasting, the label is the aggregated parking lot load, while various external conditions are used as features. The external conditions for the load forecasting include the time of the day, the weekday, the month, various weather conditions, and other external factors. In this study, the external factors considered are the period of the semester at DTU and other calendar features such as information about public holidays in Denmark.

Decision Trees

Decision Trees are a common machine learning algorithm for supervised learning problems. The algorithm can both be applied to regression tasks, as well as to classification [33]. They are used in the form of a prediction model to draw conclusions about an unknown variable. Decision trees work by recursively splitting the feature space into subsets, that are based on the values of the input features. As a result, a tree-like model is built with simple decision rules. The internal nodes of the tree represent a test of input attributes, and the following branches represents the outcome of this test. The end point of the tree, the leaf node then represents a continuous variable. An example of a simplified decision tree is shown in Figure 4.1. Here, the tree has a depth of three, meaning that there are three decisions made in the forecasting process. From the graphic it can be seen, that there are simple decision rules that the tree uses to forecast the parking lot load. In the first decision, the tree would consider if it is a working day or not. In case it is, it would continue to do further tests regarding the working hours, season and the type of the following day. In case it is not a working day, other tests are made regarding holiday periods and weekend. Finally, every node ends with a deterministic value of load.

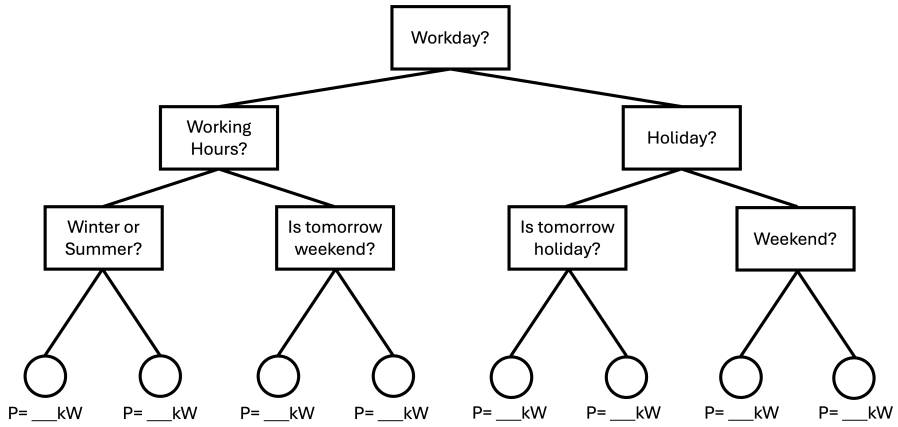

Figure 4.1: Simplified example of a decision tree

The main advantage of decision trees is that they are visually interpretable and easy to understand. Moreover, they are capable of capturing non-linear relationships between features and label without requiring significant data preparation or normalisation. Decision trees have an in-built feature selection, meaning that the tree is based on the most relevant features, while features with less relevance do not play a big role in the forecasting process. Which features are relevant, and which are not is decided in the learning process of the decision tree. However, decision trees also have considerable drawbacks. Decision trees are subject to overfitting [33, 34]. This means that the learning process creates an overly-complex tree that does not generalise well to any input data. An overfitted decision tree captures the noise of the learning data, and applies it onto the predictions. Therefore, pruning of the tree is necessary to avoid making the tree too complex [34]. Pruning refers to limiting the expansion of the tree, so that it can not extend into a node for every input. The hyperparameters that can be adjusted are the maximum depth of the tree, the minimum amount of samples that are required to end up in a node to form it, and the minimum amount of samples that a node requires for it to split further. By adjusting these parameters, the complexity of the tree can be reduced. However, the tree should not turn too general, so that it still is complex enough to capture the behaviour of the parking lot charging process accurately. Additionally, decision trees are unstable, meaning that small changes in the input data lead to a completely different tree generation when it is re-trained. To overcome the drawbacks of overfitting and instability associated with decision trees, ensemble methods such as random forests can be used.

Random Forests

Random forests are an ensemble machine learning method, which means that the prediction is based on several base models, combining into one prediction [35–37]. Each unique tree of the random forest is based on a sample of the data, resulting in several slightly different decision trees. Figure 4.2 visualises the principle of random forests. Each individual tree makes a prediction based on the input data, and the output of the random forest is equal to the average prediction for regression tasks. By combining a multitude of trees, some problems of singular decision trees are overcome. The accuracy of the prediction is increased, by considering the output of many trees. Additionally, the risk of overfitting is reduced and the model becomes more robust and stable. However, there are also key drawbacks. With random forests the interpretability of the model reduces, and for the user

it becomes less transparent to understand the prediction. While it is easy to understand each tree individually, the aggregation of the trees makes it difficult to trace the contributions of each tree to the overall prediction. Moreover, the increased complexity turns the model more computationally intensive, resulting in higher training and prediction time. This becomes relevant especially with larger datasets. The amount of trees used by the random forest can be adjusted with the hyperparameter *n_estimators*.

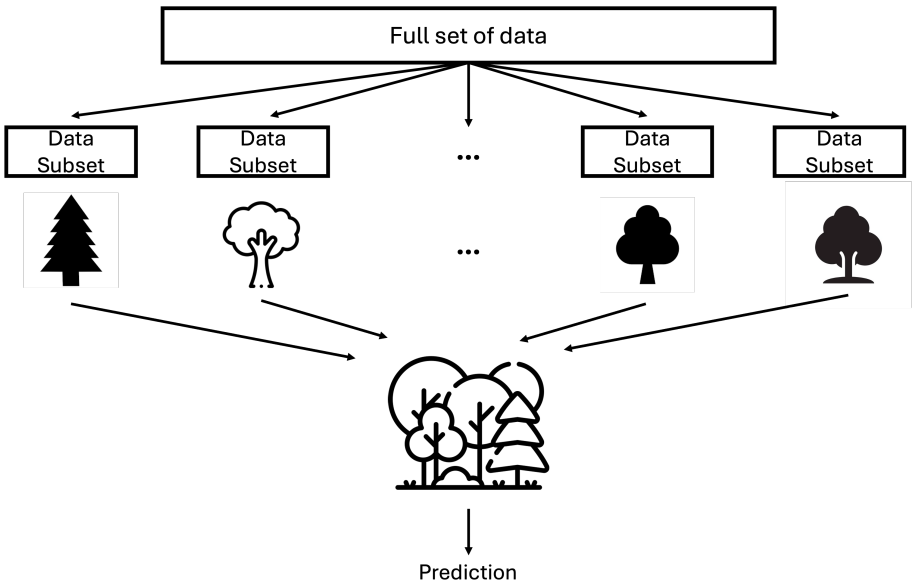

Figure 4.2: Random forest principle

Random Forest Quantile Regressor
The random forest quantile regressor can be seen as an extension to regular random forests. Conventional machine learning regressor models output one deterministic value as a prediction, which is equal to the conditional mean of the leaf nodes. However, quantile regression forests are able to output a full conditional distribution of the output variable. This is achieved by storing all predicted values from the individual trees, and considering them as a series of predictions. From this series then, quantiles can be extracted [38]. A key advantage of the random forest quantile regressor is its ability to provide additional insights into the uncertainty of the prediction. In the context of load forecasting for electric vehicles for ancillary services, this is important as it is demanded for the fluctuating resource to be available for activation 90% of the time. With a conventional random forest, this is rarely achieved as the mean value of the predictions of the individual trees is used. Using the 10^{th} quantile of the predictions corresponds to having a prediction that is available 90% of the time. *For this reason, the selected model for making load predictions is the random forest quantile regressor.*

4.1.2 Model Design and Training

The models are implemented in Python using the open-source packages scikit-learn, as well as quantile-forest [38, 39]. The label of the supervised learning model is the minute resolution load curve of the parking lot aggregation. As features, weather data from the open data platform of the Danish Meteorological Institute is used, where the data is taken from the Meteorological Observation Data API [40]. The relevant weather data features selected are:

- the precipitation

- the ambient temperature
- the visibility
- the humidity
- wind speeds

The weather station measurement point from which the observations are taken is the Copenhagen airport CPH. Even though there are weather stations that are closer to the DTU campus in Lyngby and the corresponding parking lot, the CPH airport station is selected since the dataframe has the least amount of empty datapoints and all relevant features are measured in the same location with high resolution. Weather stations closer to Lyngby do not offer all relevant features, or have dataframes with empty datapoints. The dataset has been cleaned, and measurement errors have been deleted and empty datapoints have been interpolated linearly using the previous and the upcoming datapoints in the timeseries. The temperature data is in hourly resolution, while for the wind speed, the visibility and the humidity the average value of the past 10 minutes are provided. For the precipitation, the sum of the past 10 minutes is considered. Since the data needs to be used in minute resolution, the timeseries has been resampled to match the resolution of the parking lot load curve. For this, the values have been resampled keeping the mean, except for the precipitation which has been resampled to keep the sum equal.

Moreover, calendar features such as year, month, day, and time of the day are used, along with information about public holidays in Denmark. For holidays, a binary variable *IsHoliday* is considered, which is true if the day is a holiday and false otherwise. In addition to the calendar features, case-specific information about the semester period at DTU is included. The possible options for the status of the semester period are the 13-week period, 3-week period, exam period, and holidays. Therefore, four binary variables *Is13Week*, *Is3Week*, *IsExam*, and *IsDtuHoliday* have been created. Since the calendar features are in daily resolution, they had to be resampled to minute resolution, with 1,440 repeating rows per day.

Moreover, to accurately represent the information available for the prediction, the label has been added as a feature with a lag. This is a common practice in time series forecasting. The amount of lags are chosen according to the time window before the prediction is made. Since the early FCR-D auction takes place at 00:30 on D-1, the available information from prior days has to be at least from D-2 or older. A timeline of this is shown in Figure 4.3.

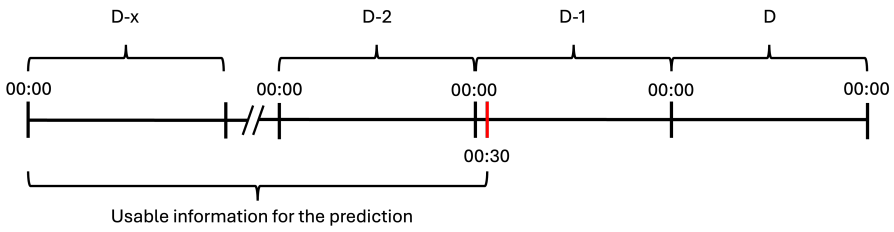

Figure 4.3: Usable information for the prediction model

The selected lags are based on the autocorrelation of the power curve. From Figure 4.4,

it can be seen that the lags with the highest auto-correlation that are available for the prediction model are 48 hours, 72 hours, 96 hours, 168 hours and 336 hours. This corresponds to 2, 3 and 4 days as well as one and two weeks prior. The lagged features are called *Load_n_h_ago*, where n is replaced with the corresponding time. The horizontal cone seen in the graphic represents the confidence level, which is set to 95% by default. If a point is outside the cone, with a confidence of 95%, there is an impact of the lag corresponding to the point.

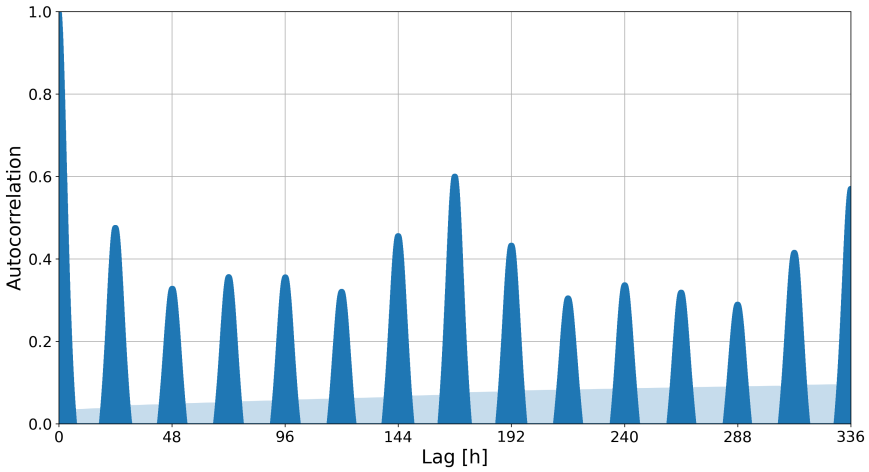

Figure 4.4: Autocorrelation of parking lot load

The same has been repeated with the variable *ChargersConnected*, so that the model not only has information about the aggregated load of n hours ago, but also about the number of connected chargers.

The final input data is then split into two parts: The majority of the input data is used for the training of the model, while the remainder is used for testing. The data is split in a way, that 70% of the complete data is used for training, and 30% are used for testing. This corresponds to a training dataset ranging from 19.09.2022 until the 11.09.2023, while the test data set ranges from 12.09.2023 until 11.02.2024. Since the maximum lag of the label as a feature is two weeks, the first two weeks of the original dataset can not be used, since the feature in this time window is not available. Therefore, for the training, these first two weeks are disregarded.

The four hyperparameters of the model are tuned using a cross-validation technique called grid search, where many combinations of hyperparameters are explored and tested. Grid search works in a way that all the combinations of hyperparameters specified are applied, and for each combination a model is trained and run. The performance of the models is then measured using metrics. The considered metrics are the mean average error (MAE), the mean squared error (RMSE) and the R^2 score, which is the coefficient of determination. As a result of the grid search, the best available hyperparameters for the model are returned.

The output of the prediction model is one timeseries with predictions that are made with a prediction horizon of 48 hours, called P_t^{pred48}*, and one with a prediction horizon of 24*

hours called P_t^{pred24}.

4.2 Decision Model

The predictions from the forecasting model are given to the decision model, to optimally allocate the available resources to the different frequency services. The decision model is based on a rolling-horizon linear programming approach, whose objective is to maximise the expected profit. Moreover, the decision is operated in two stages, one for the late auction and one for the early auction. The reason for the split into early and late auction is, that the amount of information that is available is different for the two auctions due to their timing. The model for the early and late auction is run once per day, with the additional information that is available for the relevant timepoint.

4.2.1 Early auction

The model for the early auction is shown below. The parameters that are given to the model are the price expectations for FCR-D up and down, the price expectation for FFR, and the upwards and downwards capacities C_t^{up} and C_t^{down}. The capacities are determined as follows:

$$\begin{aligned} C_t^{up} &= P_t^{pred48} \\ C_t^{down} &= \lceil P_t^{pred48} / 7.61\,\text{kW} \rceil \cdot 11kW - P_t^{pred48} \end{aligned} \tag{4.1}$$

From Equation 4.1, it can be seen that the upwards capacity is equal to the predicted load, as the chargers can reduce the demand down to 0 kW for a short time period. The downwards capacity is equal to the maximum load that the chargers can increase their demand to. However, since it is unknown how many chargers are connected, first, an amount of connected chargers for the predicted load is determined. This assumption is based on the average load per charger of the parking lot aggregation, which is 7.61 kW. Therefore, using a ceiling function which rounds up the division of the predicted load to the next integer, representing the estimated number of connected chargers. This number is then scaled with 11 kW which is the capacity per charger. Finally, since the chargers increase from the predicted load to the maximum loading, the predicted load is subtracted. As a result, C_t^{down} represents the difference between the predicted load and the estimated maximum load.

The objective function in Equation 4.2 aims to maximise the expected profit π_{exp} for an EV aggregator, by adjusting the decision variables p_t^{up-e}, p_t^{down-e}, $p_t^{FFR-prelim}$, aux_t^{up} and aux_t^{down} for all the 24 hours of the day. These variables correspond to the bids for FCR-D up, FCR-D down and FFR, where -e denotes the early auction and auxiliar variables used for constraint linearisation. The model finds the maximal expected profit based on expected prices. According to subsection 3.2.3, the price expectation for FFR is based on the hourly prices for the early auction of from the previous day. The hourly FFR price expectation is based on the projected demand two days ahead from Energinet, as described in subsection 3.2.4. It is important to consider that the bid for FFR is considered preliminary, since at the time of the early FCR-D auction at 00:30, the binding FFR demand is not public yet. However, the demand forecasts two days ahead, already giving an indication whether FFR is requested.

$$\max_{\delta \in \mathcal{D}} \pi_{exp} = \sum_{t=1}^{24} \left(p_t^{up-e} \cdot \lambda_t^{up-e} + p_t^{down-e} \cdot \lambda_t^{down-e} + p_t^{FFR-prelim} \cdot \lambda_t^{FFR} \right) \tag{4.2}$$

where the decision variables δ are formulated as a set $\mathcal{D}$:

$$\mathcal{D} = \{p_t^{up-e}, p_t^{down-e}, p_t^{FFR-prelim}, aux_t^{up}, aux_t^{down}, y_t^{up}, y_t^{down}\}$$

The model is subject to various constraints. Equation 4.3 ensures that the volumes offered in the bids are only positive or null. The two constraints in Equation 4.4 restrict the bids to the available capacities. Here, the sum of the two services that provice up-regulation to the system FR-D up and FFR need to be smaller than the forecasted parking lot up-regulation capacity C_t^{up}, while FCR-D down needs to be smaller than the down regulation capacity C_t^{down}.

$$p_t^{up-e}, p_t^{down-e}, p_t^{FFR-prelim} \geq 0 \qquad \forall t \tag{4.3}$$

$$\begin{aligned} \sum p_t^{up-e} + p_t^{FFR-prelim} &\leq C_t^{up} \qquad \forall t \\ p_t^{down-e} &\leq C_t^{down} \qquad \forall t \end{aligned} \tag{4.4}$$

Equation 4.5, 4.6 and 4.7 combined ensure that the LER regulation is considered. This means that 20% of the FCR-D bids in the opposite direction need to be reserved for battery management. However, the constraint needs to be linearised using auxiliary variables aux_t^{up} and aux_t^{down}, as a linear program only allows for linear constraints. The constraints 4.5 and 4.6 are implemented in the same way, therefore only 4.5 is explained in detail, nevertheless the same logic applies to the downwards regulation in 4.6.

Due to the LER regulation, the bid volumes for FCR-D up depend on the bid volume of FCR-D down, and the other way around respectively. However, in case that 20% of the bid for FCR-D up- or down is larger than the capacity in the other direction, the resulting maximum offer volume would be negative, which is constrained by Equation 4.3. In this case, the model would turn infeasible. Therefore, the auxiliary variables aux_t^{up} are introduced to linearise a maximum function, taking a value of either 0 or the upwards capacity C_t^{up} minus 20% of the bid for FCR-D down p_t^{down-e}. The linearisation is achieved by using four constraints. Firstly, 4.5a ensures that aux_t^{up} is larger or equal than $C_t^{up} - 0.2p_t^{down-e}$. 4.5b ensures that aux_t^{up} is larger than 0. The next two constraints work inversly by making use of a binary variable y_t^{up}, and M, which is a big number. In case y_t^{up} is 0, aux_t^{up} needs to be smaller than the sum of the big number M and $C_t^{up} - 0.2p_t^{down-e}$. If y_t^{up} takes a value of 1, aux_t^{up} needs to be smaller than M. As a result, aux_t^{up} can only take two values: either 0 or $C_t^{up} - 0.2p_t^{down-e}$. In Equation 4.7, it is then ensured that the offers are smaller than the corresponding maximum capacity determined by the auxiliary variables.

$$aux_t^{up} \geq C_t^{up} - 0.2p_t^{down-e} \tag{4.5a}$$
$$aux_t^{up} \geq 0 \tag{4.5b}$$
$$aux_t^{up} \leq C_t^{up} - 0.2p_t^{down-e} + M(1 - y_t^{up}) \tag{4.5c}$$
$$aux_t^{up} \leq My_t^{up} \tag{4.5d}$$

$$
\begin{aligned}
aux_t^{down} &\geq C_t^{down} - 0.2p_t^{up-e} \\
aux_t^{down} &\geq 0 \\
aux_t^{down} &\leq C_t^{down} - 0.2p_t^{up-e} + M(1 - y_t^{down}) \\
aux_t^{down} &\leq My_t^{down}
\end{aligned}
\tag{4.6}
$$

$$
\begin{aligned}
p_t^{up} &\leq aux_t^{up} \\
p_t^{down} &\leq aux_t^{down}
\end{aligned}
\tag{4.7}
$$

Lastly, the constraint in Equation 4.8 ensure that the bids can not be larger than the capacity that is demanded by Energinet. This constraint is mainly relevant for FFR, since in the majority of hours FFR is not requested, ensuring that the model only makes a bid for FFR in case it is necessary. The notation for the FFR demand in the early auction shows the two day ahead demand forecast by Energinet.

$$
\begin{aligned}
p_t^{up-e} &\leq D_t^{up-e} \qquad \forall t \\
p_t^{down-e} &\leq D_t^{down-e} \qquad \forall t \\
p_t^{FFR} &\leq D_t^{FFR-d2} \qquad \forall t
\end{aligned}
\tag{4.8}
$$

4.2.2 Late auction

For the late auction, predictions based on information closer to the day of operation can be used. As the late auction is held at 18:00 and the FFR auction is held at 15:00, the model for the late auction makes a combined offer for both the late FCR-D and the FFR auction. Since the gate closure time is at 15:00, the last full hour that can be used before the deadline is from 13:00 to 14:00. Therefore, the predictions from 00:00 to 14:00 can be based on lagged features with 24 hours, while the hours from 14:00 to 24:00 need to be based on predictions that are made with lagged features from D-2 with at least 48 hour lags. This is visualised in Figure 4.5.

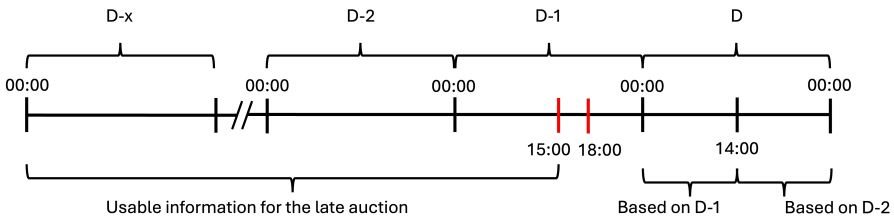

Figure 4.5: Usable information for the predictions in late auction

The decision model for the late auction, is mostly the same as for the early auction. However, there are some differences, which are highlighted below:

The objective function has been changed to optimise the bidding for the late auction, which is denoted by the -l notation. Moreover, at the time of the FFR auction at 15:00,

information about the binding FFR demand is available. Therefore, p_t^{FFR} is not preliminary anymore.

$$\max_{\delta \in \mathcal{D}} \pi_{exp} = \sum_{t=1}^{24} \left(p_t^{up-l} \cdot \lambda_t^{up-l} + p_t^{down-l} \cdot \lambda_t^{down-l} + p_t^{FFR} \cdot \lambda_t^{FFR} \right) \tag{4.9}$$

where the decision variables δ are formulated as a set $\mathcal{D}$:

$$\mathcal{D} = \{p_t^{up-l}, p_t^{down-l}, p_t^{FFR}, aux_t^{up}, aux_t^{down}, y_t^{up}, y_t^{down}\}$$

Additionally, new parameters are introduced and some existing parameters are changed. According to the analysis in section 3.2, the price expectations for FCR-D in the late auction λ_t^{up-l} and λ_t^{down-l} are based on the electricity spot prices as described in equations 3.4 and 3.5.

The available capacities for up and down regulation in the late auction are based on the load predicted with the 24 hour and 48 hour prediction horizon P_t^{pred24} and P_t^{pred48}. For this, the capacities considering the 24 hour prediction horizon are calculated:

$$\begin{aligned} C_t^{up-24} &= P_t^{pred24} \\ C_t^{down-24} &= \lceil P_t^{pred24} / 7.61\,kW \rceil \cdot 11kW - P_t^{pred24} \end{aligned} \tag{4.10}$$

However, the already offered volumes from the early auction need to be subtracted, finding the remaining capacity C_t^{up-rem} and $C_t^{down-rem}$ accordingly:

$$\begin{aligned} C^{up-rem} &= C_t^{up24} - p_t^{up-e} - 0.2 \cdot p_t^{down-e} \\ C^{down-rem} &= C_t^{down24} - p_t^{down-e} - 0.2 \cdot p_t^{up-e} \end{aligned} \tag{4.11}$$

The model is then bound to the following constraints:

$$p_t^{up-l}, p_t^{down-l}, p_t^{FFR} \geq 0 \qquad \forall t \tag{4.12}$$

$$\begin{aligned} \sum p_t^{up-l} + p_t^{FFR} &\leq aux_t^{cap-up} \qquad \forall t \\ p_t^{down-l} &\leq aux_t^{cap-down} \qquad \forall t \end{aligned} \tag{4.13}$$

$$\begin{aligned} aux_t^{up} &\geq C_t^{up-rem} - 0.2 p_t^{down-l} \\ aux_t^{up} &\geq 0 \\ aux_t^{up} &\leq C_t^{up-rem} - 0.2 p_t^{down-l} + M(1 - y_t^{up}) \\ aux_t^{up} &\leq M y_t^{up} \end{aligned} \tag{4.14}$$

$$\begin{aligned} aux_t^{down} &\geq C_t^{down-rem} - 0.2 p_t^{up-l} \\ aux_t^{down} &\geq 0 \\ aux_t^{down} &\leq C_t^{down-rem} - 0.2 p_t^{up-l} + M(1 - y_t^{down}) \\ aux_t^{down} &\leq M y_t^{down} \end{aligned} \tag{4.15}$$

$$\begin{aligned} p_t^{up-l} &\leq aux_t^{up} \\ p_t^{down-l} &\leq aux_t^{down} \end{aligned} \tag{4.16}$$

For the late auction model, the binding FFR demand is used, which is based on the binding day ahead FFR demand forecast by Energinet.

$$\begin{aligned} p_t^{up-l} &\leq D_t^{up-l} \qquad \forall t \\ p_t^{down-l} &\leq D_t^{down-l} \qquad \forall t \\ p_t^{FFR} &\leq D_t^{FFR-d1} \qquad \forall t \end{aligned} \tag{4.17}$$

4.2.3 Decision Model with Perfect Foresight

To estimate a ceiling for the profit that can be achieved with participation in frequency markets with an aggregation of EVs, another model is used that does not consider any uncertainty, but has perfect foresight. This perfect foresight includes:

- Perfect foresight of parking lot aggregation load
- Perfect foresight of FCR-D up and down prices and volumes
- Perfect foresight of FFR prices and volumes

The parameters of the model are therefore not based on load predictions or price expectations, but on the real load and the real occuring prices and volumes. The capacity for up and down regulation are defined in Equation 4.18. Here, the capacity for down regulation depends on the real numbers of connected electric vehicles.

$$\begin{aligned} C_t^{up} &= P_t^{Load} \\ C_t^{down} &= n_t^{connected} \cdot 11\ kW - P_t^{Load} \end{aligned} \tag{4.18}$$

As a result of the perfect foresight, the decision variables can be optimised at once, without a need for an optimisation for early and late auction. The model is then formulated as follows:

$$\begin{aligned} \max_{\delta \in \mathcal{D}} \pi = \sum_{t=1}^{24} \Big(& p_t^{up-e} \cdot \lambda_t^{up-e} + p_t^{up-l} \cdot \lambda_t^{up-l} + p_t^{down-e} \cdot \lambda_t^{down-e} \\ & + p_t^{down-l} \cdot \lambda_t^{down-l} + p_t^{FFR} \cdot \lambda_t^{FFR} \Big) \end{aligned} \tag{4.19}$$

with the decision variable set

$$\mathcal{D} = \{p_t^{up-e}, p_t^{up-l}, p_t^{down-e}, p_t^{down-l}, p_t^{FFR-prelim}, aux_t^{up}, aux_t^{down}, y_t^{up}, y_t^{down}\}$$

The constraints are reformulated to include both early and late auction offers at once. Constraint 4.20 ensures that all offers are positive, while 4.21 limits the offers of all up-regualation services to the upwards capacity, and all offers for downregulation to the downwards capacity.

$$p_t^{up-e}, p_t^{up-l}, p_t^{down-e}, p_t^{down-l}, p_t^{FFR-prelim} \geq 0 \qquad \forall t \tag{4.20}$$

$$\begin{aligned} \sum p_t^{up-e} + p_t^{up-l} + p_t^{FFR} \leq C_t^{up} \qquad \forall t \\ \sum p_t^{down-e} + p_t^{down-l} \leq C_t^{down} \qquad \forall t \end{aligned} \tag{4.21}$$

Constraints 4.22, 4.23 and 4.24 represent the LER constraints. Here, the only thing that changed is that both early and late auction are considered at once.

$$\begin{aligned} & aux_t^{up} \geq C_t^{up} - 0.2(p_t^{down-e} + p_t^{down-l}) \\ & aux_t^{up} \geq 0 \\ & aux_t^{up} \leq C_t^{up} - 0.2(p_t^{down-e} + p_t^{down-l}) + M(1 - y_t^{up}) \\ & aux_t^{up} \leq M y_t^{up} \end{aligned} \tag{4.22}$$

$$\begin{aligned} & aux_t^{down} \geq C_t^{down} - 0.2(p_t^{up-e} + p_t^{up-l}) \\ & aux_t^{down} \geq 0 \\ & aux_t^{down} \leq C_t^{down} - 0.2(p_t^{up-e} + p_t^{up-l}) + M(1 - y_t^{down}) \\ & aux_t^{down} \leq M y_t^{down} \end{aligned} \tag{4.23}$$

$$\begin{aligned} p_t^{up-e} + p_t^{up-l} \leq aux_t^{up} \\ p_t^{down-e} + p_t^{down-l} \leq aux_t^{down} \end{aligned} \tag{4.24}$$

Lastly, constraints in 4.25 ensure that the offer can not be larger than the demand for the corresponding service.

$$\begin{aligned} p_t^{up-e} \leq D_t^{up-e} \qquad \forall t \\ p_t^{up-l} \leq D_t^{up-l} \qquad \forall t \\ p_t^{down-e} \leq D_t^{down-e} \qquad \forall t \\ p_t^{down-l} \leq D_t^{down-l} \qquad \forall t \\ p_t^{FFR} \leq D_t^{FFR-d1} \qquad \forall t \end{aligned} \tag{4.25}$$

5 The Case

5.1 Parking Lot Description

The previously explained methodology is applied to a real-world case study. For this, the parking lot in front of building 325 at the campus of the Technical University of Denmark is considered. The parking lot consists of 6 individual chargers of the type EVlink 2S22P22R by Schneider Electric. Each charger provides two outlets for charging, resulting in 12 EVSE sockets so that 12 EVs can charge simultaneously. The maximum power per charger is 22 kW, however, each individual outlet can provide up to 13.8 kW power. Every charger is equipped with an ABB S203-C32NA circuit breaker that protects the device from overcurrents. Additionally, the whole parking lot is connected to the low voltage distribution grid via a point of common coupling (PCC). To avoid overloading of the grid connection point, the clustered parking lot is protected with a fuse. The maximum current for the entire parking lot is 99 Ampere, which equals a power of 68.59 kW according to Equation 5.1.

$$P_{PL} = \sqrt{3}IV = \sqrt{3} \cdot 99A \cdot 400V = 68.59\,kW \tag{5.1}$$

However, according to the datasheet of the fuse, an overcurrent of roughly 13% can be maintained for up to one hour, while a short-term overcurrent of approximately 30% can be maintained for minutes. The resulting parking lot powers are given by Equation 5.2.

$$\begin{aligned} P_{PL}^{1h} &= \sqrt{3} \cdot 1.13 \cdot 99A \cdot 400V = 77.505kW \\ P_{PL}^{1m} &= \sqrt{3} \cdot 1.30 \cdot 99A \cdot 400V = 89.165kW \end{aligned} \tag{5.2}$$

The charging process data of the parking lot is provided by the Electro-mobility service provider Spirii in the form of two datasets. The time range of the provided data is from 29.08.2022 until 11.02.2024, which corresponds to approximately one and a half years of data. In total, 1546 charging sessions are recorded. Once merged, the combined dataset contains various elements such as a unique transaction ID for every charging process, a charge box ID and a connector ID which contain information about the charging box and outlet used for the process, the energy charged, as well as timestamps for the start of charging and end of charging.

Out of this combined dataframe, a power curve was generated in [16], and used as a starting point for the current analysis.

Since the data does not contain power measurements and only provides energy and time, the power is extracted in a block manner, where a constant power is withdrawn through the entirety of the charging process. An illustration for such an approach is given in Figure 5.1. It can be seen, that the power of the charging process is determined by considering an equal area under both power curves, where A_1 has the same area as A_2.

$$P_{block}[kW] = \frac{E[kWh]}{t[h]} = \frac{E[kWh]}{t[s]} \cdot \frac{3600s}{h} \tag{5.3}$$

This approach introduces a shortfall, especially since the power of a charging process of an electric vehicle is non-linear and changes depending on e.g. the State of Charge (SOC) of the electric vehicles battery, which is unknown. However, as the charging power is

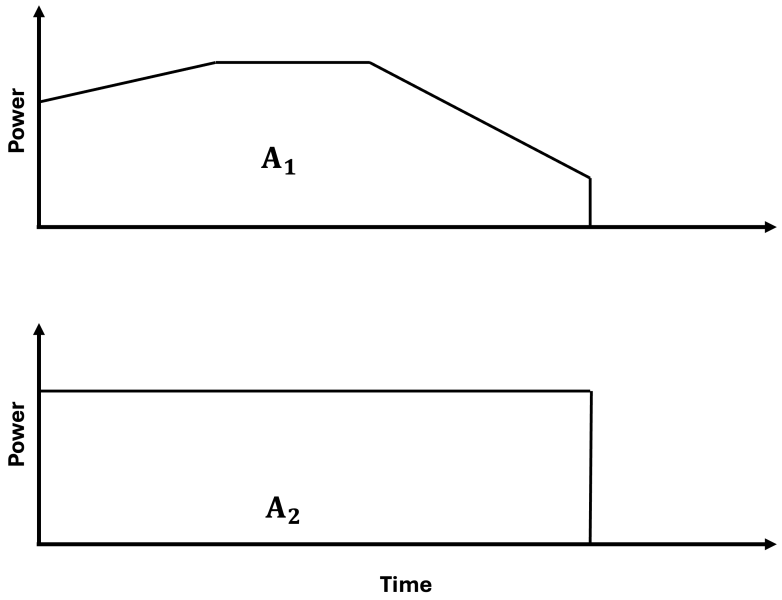

Figure 5.1: Illustration of power block curve

determined by the vehicles battery management system in an intransparent way, this is the best possible approximation. The result is a power curve for each individual charger in minute resolution.

5.2 Load Curve Analysis

An initial inspection of the load curve data shows, that in the timespan from the 29.08.2022 until the 05.09.2022, no charging processes are recorded. Therefore, the considered timerange is adjusted, as any days before the 05.09.2022 are disregarded.

The analysis of the charging sessions shows, that the average duration of a charging session is 6 hours and 5 minutes, while the average charged energy is 18.075 kWh. However, there are vast differences between the different weekdays, as shown in Figure 5.2. On the left, in Figure 5.2a it can be seen that the charging sessions on the weekends are different from the weekdays. On the weekends, the charging sessions are charging larger amounts of energy per session. However, Figure 5.2b shows that the individual sessions are shorter on the weekends. This can be explained by the fact, that on the weekends there are fewer cars charging simultaneously. Therefore, the cars that are charging can do that with a high power, while the charging power on the weekdays is limited due to higher coincidence. Thus, in moments where many cars are charging simultaneously, the power needs to be limited to prevent the parking lot from overloading the fuse. Moreover, on weekends the motivation to charge at the parking lot at DTU is different, compared to weekdays. On weekdays, the parking lot can be seen as destination charging, where users arrive to work at DTU and use the charging while the EV is parked. On the weekends, the parking lot can be seen as a charging destination, where users arrive primarily to charge, and leave as soon as possible.

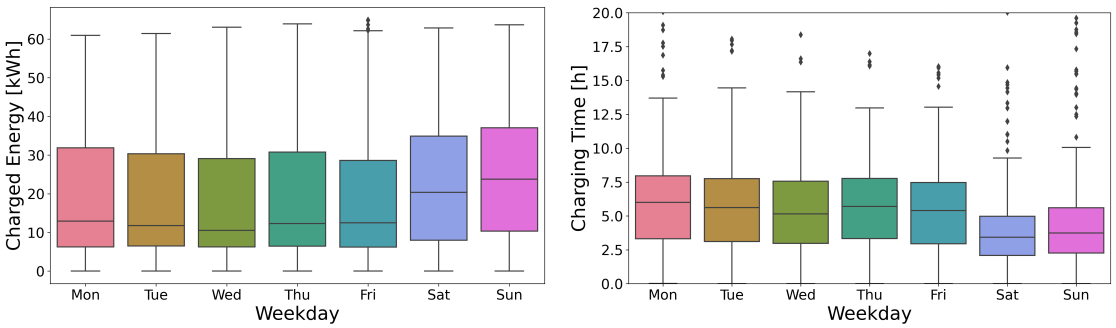

(a) Energy charged per session

(b) Charging duration per session

Figure 5.2: Boxplots per charging session

Figure 5.3 shows the accumulated energy charged for every weekday. Here, it can be seen that even though the individual charging sessions have a higher energy consumption on the weekends, the total energy charged is considerably higher on the weekdays.

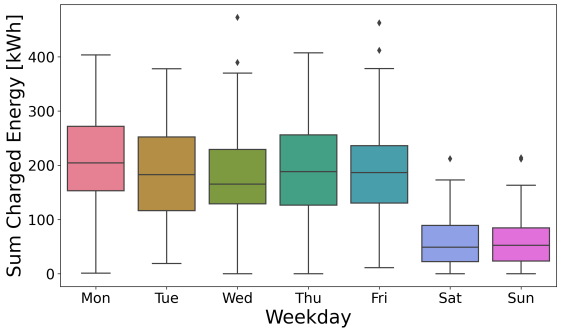

Figure 5.3: Boxplot of summed energy eharged

Additionally, a visualisation of the parking lot charging sessions as a boxplot with hourly resolution in Figure 5.4 shows that there is a difference in behaviour between working hours and non-working hours. To create the boxplot, the load curve of the aggregated 12 charging points has been grouped by weekdays and hours. In the graphic, each hourly bar represents the interquartile range from the 25^{th} quantile to the 75^{th} quantile with an indication of the mean, while the whiskers show 1.5 times the interquartile range. Outliers, which are outside of 1.5 times the interquartile range are depicted as diamonds. From the boxplot, it can be seen, that the load follows the characteristics of a workspace parking lot. It can be seen, that the charging sessions mainly take place during the working hours on weekdays, while weekends and hours outside of working hours behave differently. Figure 5.4 shows, that the arrival of cars can be expected from 07:00 on weekdays, and that most cars are gone in between 17:00 and 19:00. During the evening and the night, only a few charging sessions take place, as it can be seen that every charging is considered an outlier. Moreover, the behaviour on weekend days is different, where charging sessions start later and end earlier, in a range from 10:00 to 17:00. Considering the magnitude of load, it can be seen that the daily peak is around 09:00, after which the load decreases until the afternoon. On weekends, the load is significantly lower. Furthermore, it can be seen that the load of the cluster never exceeds 90 kW, and only exceeds the fuse limit for constant load of 68.5 kW in outliers, which validates the characteristics of the fuse.

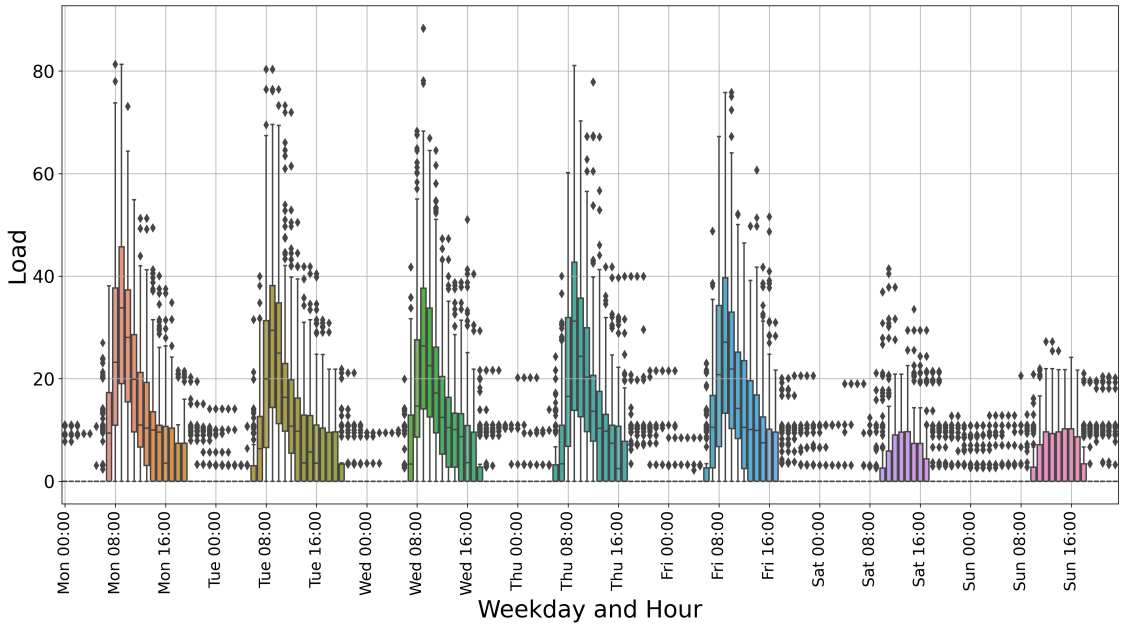

Figure 5.4: Hourly charging load boxplot

5.3 Creation of Artificial Parking Lots

To simulate the behaviour of an aggregator, the load curve of the single parking lot is used to create 30 artificial parking lots, each one with 12 outlets and similar charging patterns. As a result, 360 outlets are considered in the aggregation. For the creation of artificial parking lots, every single charging process from the real data is considered and modified in their starting and ending time with a time shift. The time shift that is applied to the charging process is based on a normal distribution with a standard deviation of 60 minutes.

The aggregation with the time shift has beneficial effects onto the 10^{th} quantile of the parking lot load, which is referred to as the *baseline*. As seen in Figure 5.5, for the single parking lot the majority of hours the baseline of the load is 0kW. It can be seen, that even for the working hours on the weekdays, the baseline does not cover a load of the parking lot. The reason for the low baseline in the individual parking lot are mostly moments, where unexpectedly no cars are charging at all. As shown in the heatmap with the 30 aggregated parking lots in Figure 5.6, the working hours are covered to a larger extend. Due to the introduced time shift, the amount of hours with no load are reduced. From Monday to Friday, the morning hours from 8:00 to 12:00 have a value for their 10^{th} quantile. However, comparing the maximum value of 255 kW with the installed capacity of 30 times 12 outlets with 11 kW each, it shows that the baseline is low.

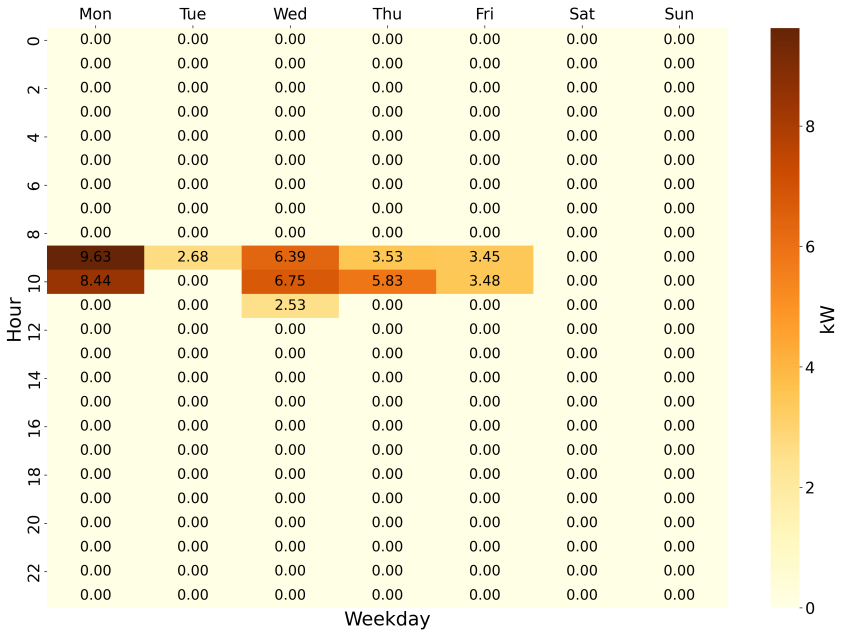

Figure 5.5: Single parking lot baseline

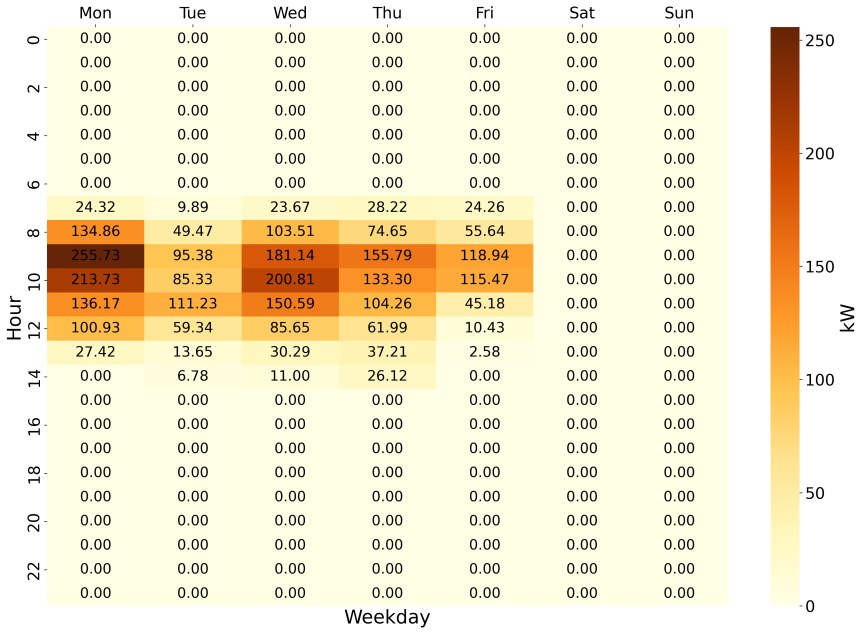

Figure 5.6: 30 aggregated parking lots baseline

6 Results

The following chapter provides the results of the analysis. Firstly, the baseline results are presented, which are only based on historical statistics. Secondly, the results based on load forecasting with the machine learning model are shown. Afterwards, a hypothethical market structure is explored, model adjustments are explained and the corresponding results are given. Lastly, a revenue ceiling is given as the result of a model with perfect foresight.

6.1 Baseline Results

To create a benchmark for the results, firstly a case is considered where the bidding is based only on historic statistical quantiles without considering any forecasting. For this, the minute resolution load curve of the 30 aggregated parking lots is expressed as the hourly 10^{th} quantile per weekday, as shown in Figure 5.6. As Energinet allows for offers which are available with a likelihood of at least 90%, the 10^{th} quantile is selected. This baseline is used as the input parameter to the optimisation. Then, for every day, the rolling horizon optimisation is run. The model decides how to allocate the available capacity to the frequency services in the early auction. In the late auction, the model has the opportunity to correct the bids from the early auction. However, as the baseline is not dynamic and consists of fixed volumes, there are not any additional capacities expected for the late auction. Therefore, there is only one possible scenario on how FCR-D can be offered in the late auction, and it happens when the model reserves capacity for FFR in the early auction based on the D-2 demand forecast from Energinet, that might not be truly demanded in the auction based on the binding D-1 forecast. Therefore, the case can occur that volume is reserved for FFR, but is then used for FCR-D.

By using the baseline, a profit of 2053.47 €can be achieved in the time period from the 12^{th} September 2023 to the 11^{th} February 2024, which corresponds to 150 days. The profit broken down into the early and late auction can be seen in Table 6.1. From the table it can be seen that the majority of the profit is generated with the FCR-D up service.

	FCR-D up	FCR-D down	FFR	Sum
Early	1385.40 (67.47%)	622.71 (30.30%)		
Late	17.73 (0.87%)	12.74 (0.63%)	14.89 (0.73%)	
Sum	1403.13 (68.34%)	635.45 (30.93%)	14.89 (0.73%)	2053.47 (100%)

Table 6.1: Profit from frequency services using the baseline [€]

Table 6.2 shows the offered capacities for the various frequency services. It is to be noted, that the offer for FFR that is listed in the early auction in the table does not actually represent an offered volume, but rather a preliminary reserved capacity. Therefore, it is marked with an asterisk, and is not included in the summation. The offered value, that is listed in the row for the late auction represents the true offered volume. From the table we can see that the described possibility to offer FCR-D in the late auction is used. It shows that the reservation volume for FFR in the moment of the early auction is larger than the volume that was truly offered. This indicates, that the model decides

to reserve capacity for FFR participation in the early auction, based on the 2 day ahead FFR demand forecast from Energinet. The smaller volume indicates that a share of the reserved volume, was not demanded anymore according to the binding day ahead FFR demand forecast by Energinet. The volume for that was initially reserved for FFR is then offered for FCR-D in the late auction instead.

	FCR-D up	FCR-D down	FFR
Early	61.43	20.54	1.00*
Late	1.41	2.499	0.67
Sum	62.09	27.57	0.67

Table 6.2: Capacities offered for frequency services using the baseline [MW]

The profit in the time period of 150 days from September to February corresponds to a linearly scaled up yearly profit of

$$2053.47\text{€} \cdot \frac{365 \text{ days}}{150 \text{ days}} = 4996.77\text{€/year}$$

Which corresponds to a yearly profit per charger of

$$\frac{4996.77\text{€/year}}{360\text{chargers}} = 13.88\text{€/charger/year}$$

6.2 Results using Load Forecasting

The analysis of the performance metrics of the predictions of the machine learning model with a prediction horizon of 24 and 48 hours shows only small differences in terms of accuracy. In Table 6.3, the performance metrics of the forecasts are shown. From the MAE, it can be seen that the model has an average error of 104.91 or 102.64 kW. Considering the significantly larger RMSE, it can be seen that the predictions that are further away from the real load are counted with a heavier weight. Therefore, it can be seen that the model tends to have larger deviations in some of its predictions. This indicates that while the average error remains moderate, there are instances where the model's predictions significantly deviate from the actual values.

Prediction Horizon	MAE [kW]	RMSE [kW]	R^2 [p.u.]
48h	104.91	195.533	0.5433
24h	102.64	191.362	0.5626

Table 6.3: Performance metrics for 24 and 48 hour prediction horizon

Figure 6.1 shows the 10^{th} quantile load prediction for the parking lot aggregation for a representative week, based on a 24 and 48 hour forecast horizon. The plot starts with Monday and ends on Sunday. From the figure, it can be seen that the two predictions do not show a lot of differences. Throughout the week, they have the same shape and only in few minutes of the week there are significant deviations between the two. It can be seen, that the models predict a daily load during the working hours, which falls to 0 kW in the afternoon and remains at 0 kW during the night. On the weekend of this week, the model does not predict that any cars are charging with a probability of more than 90%.

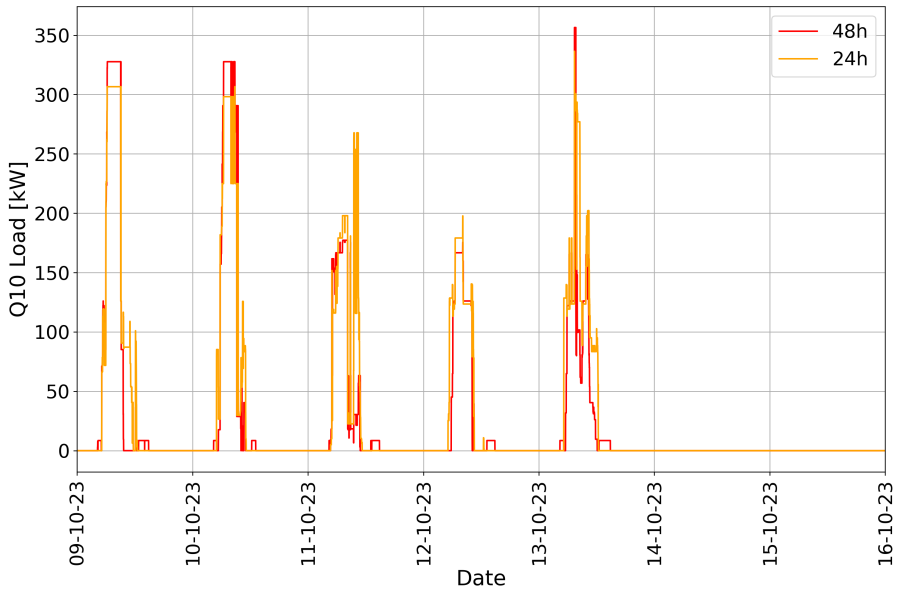

Figure 6.1: 10^{th} quantile load prediction for a representative week

The decision model optimally allocates the predicted capacities to the FCR-D up and down and FFR services based on the price expectations. In the time span from the 12.09.2023 to the 11.02.2024, the profit that can be made with participation in frequency services is 3749.37€. Compared to the baseline model, the model has an additional possibility for using the late auction. Due to the forecasts with 48 and 24 hour prediction horizon, there is the possibility that the forecasted capacities for the late auction are larger than the ones in the early auction. Therefore, the additional capacity can be offered as well in the late auction.

Table 6.4 shows how the profits are broken down into the different services and auctions, as well as the respective share of the total profit. It can be seen, that the majority of the profit is achieved through participation in the early auction for FCR-D. It shows, that roughly 97% of the profit are achieved in the early FCR-D auction. Moreover, it can be seen that FCR-D up generates more than twice the profit compared to FCR-D down. The profit achieved with FFR is comparatively low, with only 0.5% of the total profits.

	FCR-D up	FCR-D down	FFR	Sum
Early	2529.17 (67.5%)	1115.43 (29.7%)		
Late	59.87 (1.6%)	24.911 (0.7%)	19.98 (0.5%)	
Sum	2589.04 (69.1%)	1140.341 (30.4%)	19.98 (0.5%)	3749.37 (100%)

Table 6.4: Profit from frequency services [€]

Moreover, Table 6.5 shows the volume offered for each service. Again, similar to the base case it can be seen, that the actually offered volume for FFR is lower than the reserved capacity. It can be seen from the table, that the volumes offered in the late auction for FCR-D are significantly lower, compared to the early auction. Reason for this, is the very

small improvement of forecast accuracy with the 24 hour prediction horizon. Since the forecast 24 hours in advance is not significantly higher, the model already uses the majority of the forecast in the early auction. Moreover, it is seen that the capacity offered for FFR is very low, even though from the ancillary service analysis in section 3.2 it showed that FFR is very profitable. The reason for the low amount of FFR bids can be explained considering the time span of the analysis, the timing for FFR demand and the working hours in which cars arrive at the parking lot to charge. FFR is mostly demanded in spring and summer, from May to October, while the time span for the study is September to February. Therefore, only in few hours of the studied period FFR is demanded. Moreover, FFR is mainly demanded in the night hours. However, the parking lot chargers are mainly used during working hours. Therefore, there is only few occurances, in which both FFR is demanded, and there are charging processes at the same time.

Moreover, it shows that the offered capacity for FCR-D up is roughly three times larger than the one of FCR-D down. This is in accordance with the assumptions made for the case. It is assumed, that a charger can decrease its consumption to 0kW , and that it can increase the consumption to the maximum load of 11 kW for a short time period. With an average charging power of 7.61 kW, this means that the average downwards regulation capacity is 3.39 kW, while the average upwards regulation capacity is 7.61 kW, which corresponds to a factor of 2.2 between the two directions. Then, due to the LER constraints, where 20% of the offer in the opposite direction need to be reserved for battery maintenance, this mismatch is reinforced.

	FCR-D up	FCR-D down	FFR
Early	114.00	36.96	1.64*
Late	5.13	4.77	1.01
Sum	119.13	41.73	2.65

Table 6.5: Capacities offered for frequency services [MW]

Table 6.6 breaks down the profit per MW offered for the considered frequency services, representing the average prices of the frequency services in hours where the model decided to bid for it. It is visible that the profit of FCR-D up and down per MW in the early auction is considerably higher, than in the late auction, due to the larger amount of volume offered in the bids.

	FCR-D up	FCR-D down	FFR
Early	22.19	30.18	
Late	11.67	5.22	19.80

Table 6.6: Profit per volume offered of frequency services [€/MW]

Nevertheless, from a comparison of the values in Table 6.6 with the average prices of the frequency services in this studied period in Table 6.7, it is apparent that there are mismatches in the late auction, while the early auction is similar in terms of price. From the table, it can be seen that the general expectation is that the late auction provides higher revenues. Yet, it is found, that in the hours where the forecast 24 hours in advance was larger than the one 48 hours in advance, resulting in a possibility to participate in the late FCR-D auction, the prices are comparatively low. However, there are only few hours

where volumes are offered in the FCR-D late auction or for FFR, resulting in increased random variability in the observed prices. Therefore, the deviations can be explained by the small amount of hours where volumes are offered in the late auction.

	FCR-D up	FCR-D down	FFR
early	20.94	31.85	
late	27.76	39.58	90.54

Table 6.7: Average prices for frequency services in the time span from 12.09.2023 to 11.02.2024 [€]

Scaling the profits of the time span to a full year, results in a yearly profit of

$$3749.37\,€ \cdot \frac{365 \text{ days}}{150 \text{ days}} = 9122\,€/\text{year}$$

Considering that in the 30 parking lots with 12 outlets each, a resulting 360 outlets are used for the service, a profit of

$$\frac{9122€/\text{year}}{360\text{chargers}} = 25.38€/\text{charger/year}$$

can be estimated.

Nevertheless, the utilisation of the chargers is low due to the large time interval between the time of the forecast and the operation. Figure 6.2 shows the baseline, the 10^{th} quantile of the predicted capacities and the load that occured for a representative week. It can be seen, that the usable capacity from the prediction is larger than than the baseline, indicating that the machine learning approach brings benefits to the participation in frequency services. However, the difference between the 10^{th} quantile of the prediction and the actual load is large, showing that the majority of the available capacity remains unused. Therefore, section 6.3 investigates a hypothetical market structure with intraday components that benefit the utilisation of electric vehicles providing frequency services, since the aggregator is able to make offers closer to real time.

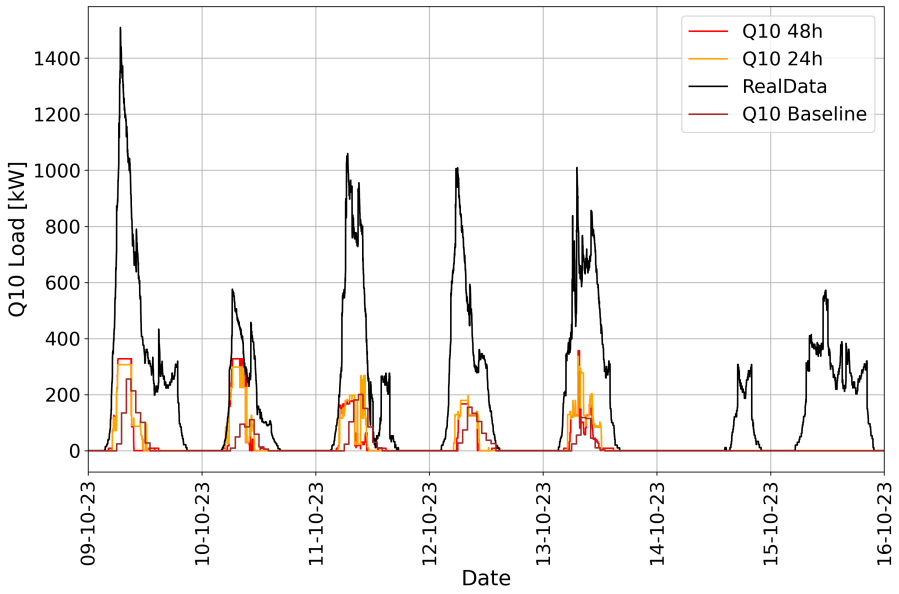

Figure 6.2: 10^{th} quantile load prediction, baseline and real load for a representative week

6.3 Results under a Hypothetical Market Structure

Table 6.8 can be seen as an extension of Table 6.3. From the table, it is visible that the accuracy of the load forecast improves significantly, when the prediction horizon moves close to real time operation. The metrics show that the MAE is 104.91 kW when considering a 48 hour prediction horizon, which reduces to less than half of it when the prediction horizon is only 1 hour. Nevertheless, the RMSE remains higher than the MAE, indicating that the model continues to make predictions that are occasionally largely off from the true values. Lastly, the R^2 metric, which describes the coefficient of determination of the prediction, increases as well with shorter prediction horizons. This indicates that the model is more effective at capturing the variance in the target variable when forecasting closer to real time.

Prediction Horizon	MAE [kW]	RMSE [kW]	R^2 [p.u.]
48h	104.91	195.533	0.5433
24h	102.64	191.362	0.5626
2h	79.61	154.164	0.7161
1h	47.66	100.385	0.8800

Table 6.8: QuantileForestRegressor performance metrics for different time horizons

As a result of the higher accuracy with shorter prediction horizon, the forecast allows for higher loads to be forecasted with the 10th quantile, resulting in larger capacities for frequency services. For the previously shown representative week, the figure is updated to include the predictions with a horizon of 2h and 1h. From the figure, it can be seen that the predictions are significantly closer to the real load.

Figure 6.4 shows how the average 10th quantile prediction of load changes with the different time horizons. It can be seen, that the orange and the red curve representing the 24 and 48 hour prediction horizon respectively, are equal or similar in magnitude for the majority of hours. However, with shorter time horizons for the predictions, the blue and green

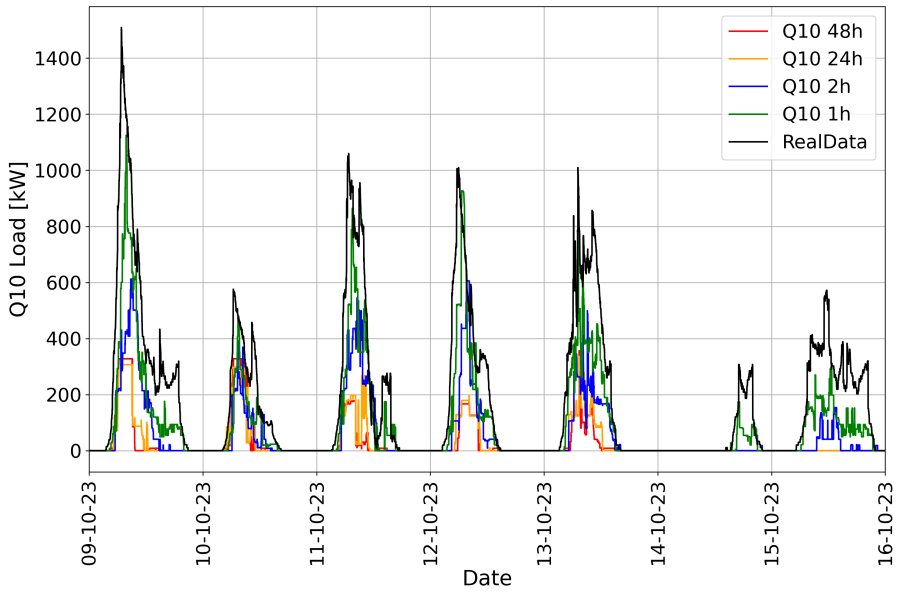

Figure 6.3: 10th quantile load prediction with shorter time horizon and real load for a representative week

curves however are higher for all hours.

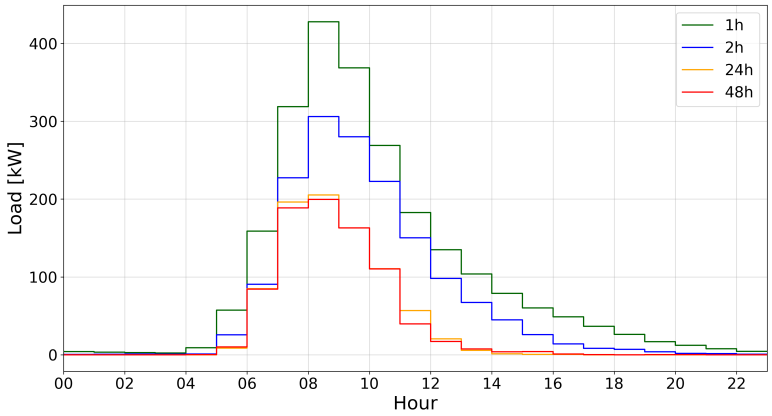

Figure 6.4: Mean hourly load forecast with different time horizons

Therefore, a hypothetical market structure for FCR-D and FFR is investigated where the gate closure times are modified. The considered gate-closure times are shown below in Table 6.9. The major changes are, that the early FCR-D auction moves together with the FFR auction at 15:00, while the late auction is converted into an intraday format with hourly auctions and a gate-closure time of H-1. As a consequence, the forecast with a two hour prediction horizon is used for the late FCR-D auction, while the early FCR-D and the FFR auctions are based on load forecasts with a prediction horizon of 48 hours. The timeline of gate-closure times and usable information for the predictions is shown in Figure 6.5. This hypothetical market structure is from now on referred to as ”Intraday FCR-D Late”.

Service	Gate-closure	Auction type
FCR-D up/down early	D-1 15:00	Day-ahead
FCR-D up/down late	D H-1	Intraday
FFR	D-1 15:00	Day-ahead

Table 6.9: Gate closure times for frequency service markets with intraday FCR-D late

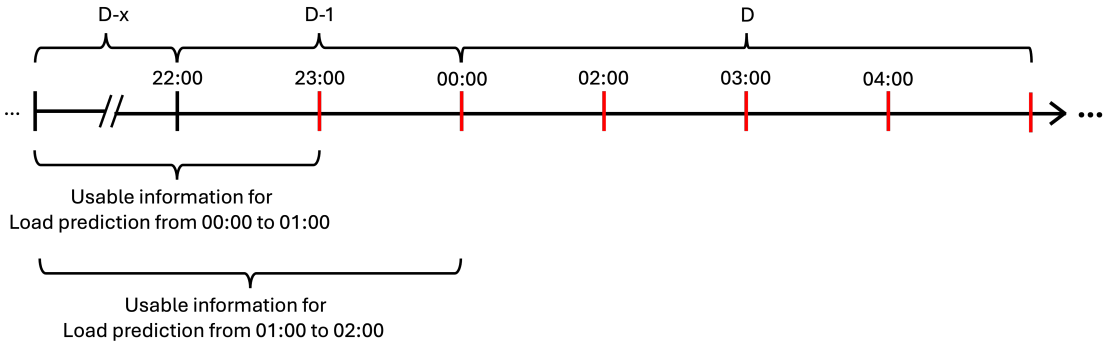

Figure 6.5: Usable information for FCR-D late auction under intraday FCR-D late scheme

With the new structure the machine learning prediction model is extended with an additional lag, where the label with a lag of 2 hours is used as a feature. Moreover, the parameters for decision model need to be adjusted accordingly: The available capacities C^{up-rem} and $C^{down-rem}$ are different for the late auction. The early auction remains as before, with the capacities based on the predictions of 48 hours in advance. For the late auction however, the capacities are based on P_t^{Pred2}, the predictions 2 hours in advance, respecting the hypothetical gate-closure time. Then, the remaining capacity for the late auction is determined by subtracting the already offered bids from the capacity. Moreover, in this scheme the binding demand for FFR D_t^{FFR-d1} is already available for the early auction. Therefore, in the early auction p^{FFR} is not preliminary, but binding.

$$\begin{aligned} C_t^{up-2} &= P_t^{pred2} \\ C_t^{down-2} &= \lceil P_t^{pred2}/7.61\,kW \rceil \cdot 11kW - P_t^{pred2} \end{aligned} \tag{6.1}$$

$$\begin{aligned} C^{up-rem} &= C_t^{up2} - p_t^{up-e} - 0.2 \cdot p_t^{down-e} \\ C^{down-rem} &= C_t^{down2} - p_t^{down-e} - 0.2 \cdot p_t^{up-e} \end{aligned} \tag{6.2}$$

The offered volumes for each service and auction is shown in Table 6.10. From the table it becomes clear, that the addition of the possibility to offer volumes in an auction style similar to an intraday auction unlocks a large amount of flexibility to be offered in the late auction. It can be seen that in the late auction, the amount of FCR-D down is more than twice as high as the amount for FCR-D up. Due to the higher average price in for FCR-D down, which is shown in Table 6.7, the model decides to offer larger quantities of down-regulation. The offered volumes for the early auction are similar to the ones of the current market structure, which corresponds to the fact that the gate-closure time of the early auction is considered to be one day before the day of operation. Moreover, it can be

	FCR-D up	FCR-D down	FFR
Early	114.03	36.95	1.59
Late	86.37	171.31	
Sum	200.40	208.26	1.59

Table 6.10: Capacities offered for frequency services under hypothetical scheme [MW]

seen that the volume for FFR remains low, due to the aforementioned mismatch between the demand hours for FFR and the operating hours of the workspace parking lots.

Table 6.11 shows how the offered volumes translate into profits, broken down into the different services and auctions. In total, a profit of 11,522.23 €is achieved with the participation in frequency services, which is roughly **three times** as much as under the current market structure. The majority of the profits is generated in the late auction, where 68.14% of the profits originate from. It can be seen that more than half of the earnings are realised with the FCR-D up service, while 44.2% are realised with FCR-D down. Comparing this to the volumes offered in Table 6.10, it is noticeable, that FCR-D up generates more profit with less capacity.

	FCR-D up	FCR-D down	FFR	Sum
Early	2528.946	1115.866	25.022 (0.2%)	3669.83
	(21.95%)	(9.70%)		(31.85%)
Late	3874.710	3977.689		7852.399
	(33.62%)	(34.52%)		(68.14%)
Sum	6403.656	5093.555	25.022 (0.2%)	11522.23
	(55.5%)	(44.2%)		(100%)

Table 6.11: Profit from frequency services with hypothetical market scheme [€]

A calculation of the profits per capacity in Table 6.12 show, that the profit per volume is larger and closer to the average prices in the corresponding time span. This can be explained by the larger amount of hours with participation in the FCR-D late auction, reducing the variance in realised prices. Nevertheless, the amount of hours with participation in FFR is low. Therefore, there are still considerable mismatches in average prices and FFR prices in hours where the model offered FFR.

	FCR-D up	FCR-D down	FFR
Early	22.19	30.18	
Late	44.86	23.21	15.63

Table 6.12: Profit per volume offered of frequency services in intraday late auction scheme [€/MW]

Scaling the results to a whole year of operation, the yearly profit is found as

$$11522.23\ € \cdot \frac{365\ \text{days}}{150\ \text{days}} = 28,039.3\ €/\text{year}$$

Which corresponds to a yearly profit per charger of

$$\frac{28,039.3\ €/\text{year}}{360\ \text{chargers}} = 77.89\ €/\text{charger/year}$$

6.4 Results with Perfect Foresight

Under perfect foresight, the model optimally allocates the available capacities to the different services. This means, that for every hour a value is found, where 90% of the minute-resolution load is higher than the offered value. It is found that the profit with perfect foresight is 26065.08 €in the considered time span from September to February. The breakdown of profits per service can be seen in Table 6.13. From the table it shows that for the parking lot aggregation, FCR-D up is the most profitable service, with a contribution of almost 80% of the total profit. It can also be seen, that FCR-D down achieves more profit in the early auction, whereas FCR-D up is mostly offered in the late auction. It shows, that FFR has a very low contribution to the overall profits.

	FCR-D up	FCR-D down	FFR	Sum
Early	7157.83 (27.46%)	3496.71 (13.42%)		
Late	13544.88 (51.97%)	1582.40 (6.07%)	283.26 (1.08%)	
Sum	20702.71 (79.43%)	5079.11 (19.49%)	282.26 (1.08%)	26065.08 (100%)

Table 6.13: Profit from frequency services under perfect foresight [€]

Table 6.14 reveals that the volumes offered in the late auction are significantly lower than in the early auction. For FCR-D up, more than twice the capacity is offered in the early auction compared to the late auction, while the profits in the late auction are drastically higher. The same applies to FCR-D down, where the volume offered in the early auction is roughly 5 times as large as in the late auction. Nevertheless, with only 24.09 MW for FCR-D down in the late auction, 6.07% of the total profit are achieved. This behaviour shows the profitability of the price spikes in the late auction.

	FCR-D up	FCR-D down	FFR
Early	319.21	118.43	6.99
Late	134.84	24.09	
Sum	454.05	142.52	6.99

Table 6.14: Capacities offered for frequency services under perfect foresight [MW]

Finally, the results are scaled to a full year showing the maximum profitability that EV aggregators can achieve with participation in frequency services:

$$26065.08\ € \cdot \frac{365\ \text{ days}}{150\ \text{ days}} = 63,425.028\ €/\text{year}$$

Which corresponds to a yearly profit per charger of

$$\frac{63,425.028\ €/\text{year}}{360\ \text{chargers}} = 176.18\ €/\text{charger/year}$$

Scenario	Baseline	Day-Ahead Predictions	Intraday Scheme	Perfect Foresight
Profit	2053.47€	3749.37€	11522.23€	26065.08€
Share of Perfect foresight profit	7.88%	14.39%	44.21%	100%

Table 6.15: Comparison between the scenarios and perfect foresight

Comparing the profitability of the baseline, the prediction model, and the intraday market structure with the one using perfect foresight in Table 6.15, it is visible that the addition of machine learning for load forecasting improves the profitability of participation in frequency services. Moreover, it is visible that a possibility to offer closer to real time, results in larger profits due to the unlocking of a large amount of flexibility that can be offered to maintain grid stability.

7 Discussion and Conclusion

Summary of Results
The thesis analyses the characteristics of a parking lot with 12 electric vehicle chargers and investigates possibilities of participating in ancillary service markets in the Nordic power system. Based on the data of the existing parking lot, artificial parking lots are generated. The generated parking lots have similar load characteristics as the existing one. The work then takes the perspective from an aggregator, combining the load of the real and artificial parking lots to participate in frequency services. Moreover, a load forecasting model has been developed to predict the electrical load of the parking lot aggregation. The load forecasting model is based on a machine learning approach, and makes use of random forests. Additionally, a decision model is developed that optimally allocates the forecasted capacity to different frequency services, namely FCR-D and FFR.

To form a baseline, the 10^{th} quantile of the daily hourly load is considered as an input to the decision model. The model offers the available capacities to both the FFR market, as well as the early FCR-D auction, and is able to correct the offers in the late FCR-D auction. It is found that by using the baseline, a very low amount is offered in the late FCR-D auction, as only unnecessarily reserved capacities for FFR can be offered. As a result, a yearly profit of 13.88 €per year per charger can be expected. The majority of the profits originate from FCR-D up, while a smaller share originates from FCR-D down in the early auction. The late FCR-D auction as well as FFR correspond to a neglectable profit.

The usage of the forecasts of the machine learning model improves the profitability to 25.38 €per year per charger. Moreover, in the late auction the model can not only correct bids with capacity that was reserved for FFR, but also offer the additional load that is forecasted at a timepoint closer to real time operation. However, it is found that the load forecast barely improves when changing from a prediction horizon of 48 hours to a prediction horizon of 24 hours. Therefore, there is a low utilisation of capacities in the late FCR-D auction. Again, the majority of profits are achieved by providing FCR-D up in the early auction, while a smaller share is generated with FCR-D down. Even though the profits from the late auction and FFR are slightly larger compared to the baseline, the profit is still neglectable.

Therefore, a hypothetical market scheme is considered, where the FCR-D late auction is held hourly on the day of operation, with a gate-closure time 1 hour before the operation. It is found that this scheme significantly increases the amount of flexibility an aggregator can offer for frequency services. As a result, the decision model offers a considerably larger amount of flexibility that is available with a likelihood of at least 90% according to the regulation from Energinet. Consequently, the profitability of the participation in the late auction improves significantly. Here, the majority of profit is achieved in the FCR-D late auction, where the up and down service contribute almost equally. Under the hypothetical scheme, a yearly profit of 77.89 €per charger can be expected.

Finally, a model with perfect foresight is developed that can estimate a maximum prof-

itability which can be used as an expectation ceiling. It is found that the maximum profitability per charger per year is 176.18 €.

From this, it is shown that the uncertainty can be addressed by applying machine learning for load forecasting. Given the forecasted capacities, an optimal allocation to different frequency services is found. Even though FFR is generally very profitable, the demand hours do not align with the charging patterns of the workspace parking lot. Therefore, only little profit can be achieved by offering FFR. Given the setup of the parking lot, underfrequency up-regulation service FCR-D up is found to be a larger source of profits compared to overfrequency down-regulation service FCR-D down.

Discussion
Nevertheless, the results should be considered carefully. The study is based on one parking lot with 12 electric vehicle chargers, which represents a small sample size. In the small sample size, every anomaly in charging behaviour, e.g. a charging process in the night or a delay in charging process on weekdays, has large impact. As the artificial parking lots are based on the real one, the anomalies are also applied on the 29 artificially created ones. The application of the time shift mitigates the issue to some extent, however, with anomalies that occur longer than 1 hour the impact is still high. The aggregation of artificially created parking lots can not directly be translated to the real world, since the chance of an anomaly in charging patterns occurring at 30 parking lots at once is very low. Therefore, the anomalies make both the 10^{th} quantile baseline as well as the machine learning forecasts less stable. It is assumed, that an aggregation of 30 real parking lots with similar characteristics has a much more stable electricity consumption. Additionally, an aggregation of parking lots at workspaces, residential chargers, and other characteristics might be combined to create a more reliable baseline.

Moreover, the study covers a time span of 150 days in the winter, where the decision model allocates the capacities to the different frequency services. The profits from the considered period are then scaled to a full year. However, as this period is in the winter, the demand for FFR is low and the prices for FCR-D are comparatively low in contrast to the spring and summer period. As a result, it can be assumed that the profitability for a full year might be higher.

Furthermore, it is debatable if an aggregation of EVs has to be considered as a limited energy reservoir. Even though an individual EV can not sustain a full FCR-D activation for two hours, an aggregation possibly can. By activating only a part of the aggregation at once, and continuing through the aggregation pool, a full activation might be possible for more than two hours. However, in this study the user convenience is prioritised, therefore, the charging process should be disturbed as little as possible. Thus, it has been decided to apply LER constraints.

Lastly, the hypothetical market structure which has the characteristic of an intraday auction for FCR-D needs to be viewed critically. On the one hand, with the current market structure the capacities that can be offered for frequency services with fluctuating resources is very limited. To draw a comparison, it is hard to imagine a world where fluctuating resources such as wind power or solar photovoltaic would have to offer their spot market offers according to a 10^{th} quantile one day before operation, without any chance of correcting on the operation day. In case that they repeatedly violate their offer, they would

be excluded from the market for a small time period. This would not only be highly ineffective, but also be a complete show-stopper for the energy transition. According to the EU, energy efficiency is a key priority, and markets need to be designed in a way that allow resources to be used efficiently. In light of the climate crisis, there is no time for wasting available carbon free resources. Moreover, the price shocks for FCR-D in Spring 2024 show that the market is far from being saturated, and that additional capacities for frequency services would be a big help in keeping electricity costs low.

On the other hand, ensuring the safe and secure operation of the system is essential. This requires maintaining sufficient capacity for frequency services at all times. Consequently, any change in market structure must be carefully evaluated, considering all potential outcomes. This assessment should include both the benefits and the risks and drawbacks associated with such changes.

Outlook
Therefore, it is recommended that future research includes an analysis of aggregating various chargers with different characteristics. Moreover, it should be considered which technologies have synergies that can be used for optimal participation in frequency services. Additionally, other flexibility services utilizing EVs should be explored, particularly focusing on how AI can help harnessing existing EV capacities. Finally, future studies might investigate other methods for successfully and efficiently integrating fluctuating resources into ancillary service markets, as well as the impact of the market changes investigated in this thesis and other potential opportunities.

Bibliography

[1] United Nations. *Climate Change 'Biggest Threat Modern Humans Have Ever Faced', World-Renowned Naturalist Tells Security Council, Calls for Greater Global Cooperation*. 2021. URL: https://press.un.org/en/2021/sc14445.doc.htm (visited on 02/16/2024).

[2] International Energy Agency. *How much CO2 does Denmark emit?* 2024. URL: https://www.iea.org/countries/denmark/emissions (visited on 02/16/2024).

[3] Mattia Marinelli. *Mattia Marinelli – Course 46740 – Distributed energy technologies modelling and control Electric vehicle technologies Course 46740 - Lecture 05*. Mar. 2024.

[4] Regeringen. *Danmark fremad – Infrastrukturplan 2035*. 2021. URL: https://www.trm.dk/publikationer/2021/danmark-fremad-infrastrukturplan-2035 (visited on 02/16/2024).

[5] International Energy Agency. *Denmark 2023 - Executive summary*. URL: https://www.iea.org/reports/denmark-2023/executive-summary (visited on 07/17/2024).

[6] Tim Unterluggauer et al. "Electric vehicle charging infrastructure planning for integrated transportation and power distribution networks: A review". English. In: *eTransportation* 12 (2022). ISSN: 2590-1168. DOI: 10.1016/j.etran.2022.100163.

[7] Tim Unterluggauer. "Urban Electric Vehicle Charging Infrastructure: Planning, Grid Impact and Grid Integration". English. PhD thesis. 2024. DOI: 10.11581/DTU.00000312.

[8] Energinet. *LONG-TERM DEVELOPMENT NEEDS IN THE POWER GRID*. URL: https://en.energinet.dk/About-our-reports/Reports/Long-term-development-power-grid/.

[9] Andrew W. Thompson and Yannick Perez. "Vehicle-to-Everything (V2X) energy services, value streams, and regulatory policy implications". In: *Energy Policy* 137 (2020), p. 111136. ISSN: 0301-4215. DOI: https://doi.org/10.1016/j.enpol.2019.111136. URL: https://www.sciencedirect.com/science/article/pii/S0301421519307244.

[10] Energinet. *OUTLOOK FOR ANCILLARY SERVICES 2023-2040*. Tech. rep. 2023.

[11] Irene Manzanares Casla, Abolfazl Khodadadi, and Lennart Söder. "Optimal Day Ahead Planning and Bidding Strategy of Battery Storage Unit Participating in Nordic Frequency Markets". In: *IEEE Access* 10 (2022), pp. 76870–76883. DOI: 10.1109/ACCESS.2022.3192131.

[12] Zeenat Hameed, Chresten Træholt, and Seyedmostafa Hashemi. "Investigating the participation of battery energy storage systems in the Nordic ancillary services markets from a business perspective". In: *Journal of Energy Storage* 58 (2023), p. 106464. ISSN: 2352-152X. DOI: https://doi.org/10.1016/j.est.2022.106464. URL: https://www.sciencedirect.com/science/article/pii/S2352152X22024537.

[13] Andreas Thingvad et al. "Economic Value of Multi-Market Bidding in Nordic Frequency Markets". English. In: *Proceedings of International Conference on Renewable Energies and Smart Technologies*. 2022 International Conference on Renewable Energies and Smart Technologies, 2022 REST ; Conference date: 28-07-2022 Through 29-07-2022. United States: IEEE, 2023. DOI: 10.1109/REST54687.2022.10023471. URL: https://ic-rest.org/.

[14] Kristian Sevdari et al. "Ancillary services and electric vehicles: An overview from charging clusters and chargers technology perspectives". English. In: *Renewable and*

Sustainable Energy Reviews 167 (2022). ISSN: 1364-0321. DOI: 10.1016/j.rser.2022.112666.

[15] Pauline Thüne and David Eduardo Menchaca Santos. "Business cases and technological trends in vehicle-to-grid applications for residential users and fleet vehicles". In: (2024). URL: https://orbit.dtu.dk/files/350941115/Thesis_Menchaca_Thuene.pdf (visited on 07/15/2024).

[16] Carlos Hermana Rivera. *Quantifying the flexibility potential of electric vehicles smart charging*. 2024. URL: https://orbit.dtu.dk/en/activities/quantifying-the-flexibility-potential-of-electric-vehicles-smart-.

[17] S. de la Torre, J.A. Aguado, and E. Sauma. "Optimal scheduling of ancillary services provided by an electric vehicle aggregator". In: *Energy* 265 (2023), p. 126147. ISSN: 0360-5442. DOI: https://doi.org/10.1016/j.energy.2022.126147. URL: https://www.sciencedirect.com/science/article/pii/S036054422203033X.

[18] Peter A. V. Gade, Henrik W. Bindner, and Jalal Kazempour. "Leveraging P90 Requirement: Flexible Resources Bidding in Nordic Ancillary Service Markets". English. In: IEEE SmartGridComm 2024 ; Conference date: 17-09-2024 Through 20-09-2024. 2024.

[19] Gustav Adelgaard Lunde and Emil Ventzel Damm DTU Wind. "The synergy effect of aggregating distributed units for FCR-D bidding optimization". In: (2024).

[20] Nils Müller et al. "On the trade-off between profitability, complexity and security of forecasting-based optimization in residential energy management systems". English. In: *Sustainable Energy, Grids and Networks* 34 (2023). ISSN: 2352-4677. DOI: 10.1016/j.segan.2023.101033.

[21] Heba-Allah I. El-Azab et al. "Seasonal electric vehicle forecasting model based on machine learning and deep learning techniques". In: *Energy and AI* 14 (2023), p. 100285. ISSN: 2666-5468. DOI: https://doi.org/10.1016/j.egyai.2023.100285. URL: https://www.sciencedirect.com/science/article/pii/S2666546823000575.

[22] ENTSO-E. *P1 – Policy 1: Load-Frequency Control and Performance [C]*. URL: https://www.entsoe.eu/fileadmin/user_upload/_library/publications/entsoe/Operation_Handbook/Policy_1_final.pdf (visited on 07/17/2024).

[23] Netztransparenz. *Sekündliche Frequenz - Sekündliche Daten*. 2024. URL: https://www.netztransparenz.de/en/Balancing-Capacity/Balancing-Capacity-data/Data-in-second-resolution (visited on 07/19/2024).

[24] FINGRID. *Datasets Frequency - historical data*. 2024. URL: https://data.fingrid.fi/en/datasets/339 (visited on 07/19/2024).

[25] Energinet. *ANCILLARY SERVICES TO BE DELIVERED IN DENMARK - TENDER CONDITIONS*. 2024. URL: https://en.energinet.dk/Electricity/Ancillary-Services/Tender-conditions-for-ancillary-services/ (visited on 07/19/2024).

[26] Jan Engelhardt et al. "Energy recovery strategies for batteries providing frequency containment reserve in the Nordic power system". In: *Sustainable Energy, Grids and Networks* 32 (2022), p. 100947. ISSN: 2352-4677. DOI: https://doi.org/10.1016/j.segan.2022.100947. URL: https://www.sciencedirect.com/science/article/pii/S2352467722001928.

[27] FINGRID. *Reserves and balancing power*. URL: https://www.fingrid.fi/en/electricity-market/reserves_and_balancing/#reserve-obligations-and-procurement-sources (visited on 07/17/2024).

[28] Elias Huuhtanen. *Turbine fault causes outage at 1.6 GW Olkiluoto 3*. 2024. URL: https://montelnews.com/news/400a09da-3c2e-4765-af6f-1a055738e7c5/turbine-fault-causes-outage-at-1-6-gw-olkiluoto-3.

[29] TenneT. *NordLink*. 2022. URL: https://www.tennet.eu/projects/nordlink (visited on 07/17/2024).
[30] Energinet. *FFR, Fast Frequency Reserve, Demand DK2*. URL: https://www.energidataservice.dk/tso-electricity/ffrdemanddk2 (visited on 07/19/2024).
[31] Svenska Kraftnät et al. *BSP - Implementation Guide: Fifty Nordic MMS - FCR capacity market*. 2023. URL: https://energinet.dk/media/xe4nuif2/implementation-guide-fcr-capacity-market-bsp.pdf (visited on 07/19/2024).
[32] Katarina Knezović et al. "Enhancing the Role of Electric Vehicles in the Power Grid: Field Validation of Multiple Ancillary Services". In: *IEEE Transactions on Transportation Electrification* 3.1 (2017), pp. 201–209. DOI: 10.1109/TTE.2016.2616864.
[33] scikit learn. *Decision Trees*. URL: https://scikit-learn.org/stable/modules/tree.html (visited on 07/02/2024).
[34] Rishika Ravindran. *Overfitting and Pruning in Decision Trees — Improving Model's Accuracy*. 2023. URL: https://medium.com/nerd-for-tech/overfitting-and-pruning-in-decision-trees-improving-models-accuracy-fdbe9ecd1160 (visited on 07/02/2024).
[35] Leo Breiman. "Random Forests." In: *Machine Learning* 45 (Jan. 2001), pp. 5–32. DOI: 10.1023/A:1010933404324.
[36] scikit learn. *Ensembles: Gradient boosting, random forests, bagging, voting, stacking*. URL: https://scikit-learn.org/stable/modules/ensemble.html (visited on 07/02/2024).
[37] Evan Lutins. *Ensemble Methods in Machine Learning: What are They and Why Use Them?* 2017. URL: https://towardsdatascience.com/ensemble-methods-in-machine-learning-what-are-they-and-why-use-them-68ec3f9fef5f (visited on 07/02/2024).
[38] Zillow Group. *quantile-forest*. URL: https://zillow.github.io/quantile-forest/index.html (visited on 07/02/2024).
[39] F. Pedregosa et al. "Scikit-learn: Machine Learning in Python". In: *Journal of Machine Learning Research* 12 (2011), pp. 2825–2830.
[40] *DMI Open Data - Meteorological Observation Data*. 2024. URL: https://opendatadocs.dmi.govcloud.dk/en/Download.

Technical
University of
Denmark

Elektrovej, Building 329
2800 Kgs. Lyngby
Tlf. 4525 1700

www.wind.dtu.dk/